

# Micromixing Within Microfluidic Devices

Lorenzo Capretto, Wei Cheng, Martyn Hill, and Xunli Zhang

**Abstract** Micromixing is a crucial process within microfluidic systems such as micro total analysis systems ( $\mu$ TAS). A state-of-art review on microstructured mixing devices and their mixing phenomena is given. The review first presents an overview of the characteristics of fluidic behavior at the microscale and their implications in microfluidic mixing processes. According to the two basic principles exploited to induce mixing at the microscale, micromixers are generally classified as being passive or active. Passive mixers solely rely on pumping energy, whereas active mixers rely on an external energy source to achieve mixing. Typical types of passive micromixers are discussed, including T- or Y-shaped, parallel lamination, sequential, focusing enhanced mixers, and droplet micromixers. Examples of active mixers using external forces such as pressure field, electrokinetic, dielectrophoretic, electrowetting, magneto-hydrodynamic, and ultrasound to assist mixing are presented. Finally, the advantages and disadvantages of mixing in a microfluidic environment are discussed.

**Keywords** Active micromixers · Microfluidics · Micromixing · Mixing principles · Passive micromixers

## Contents

1	Introduction and Outline .....	29
2	The Microfluidic Environment and Mixing Principles .....	30
2.1	Reynolds Number and Diffusion .....	30
2.2	Mixing in Microfluidic Devices .....	32
3	Micromixers .....	33
3.1	Passive Micromixers .....	33
3.2	Active Micromixers .....	51

4	Why Microfluidic Mixers?	57
5	Conclusions	59
	References	60

## Symbols

$A$	Cross-sectional area ( $\text{m}^2$ )
$Ca$	Capillary number
$D$	Diffusion coefficient ( $\text{m}^2 \text{s}^{-1}$ )
$D_h$	Hydraulic diameter (m)
$f$	Frequency of the disturbance action
$h$	Height of the channels (m)
$j$	Diffusion flux ( $\text{mol m}^{-2} \text{s}^{-1}$ )
$k$	Boltzmann's constant ( $k = 1.381 \cdot 10^{-23} \text{J K}^{-1}$ )
$n$	Number of parallel fluid substreams
$Pe$	Peclet number
$P_{\text{wet}}$	Wetted perimeter (m)
$Q_1$	Volumetric flow rates for the lateral channels ( $\text{m}^3 \text{s}^{-1}$ )
$Q_2$	Volumetric flow rates of the central inlet channel ( $\text{m}^3 \text{s}^{-1}$ )
$Q_3$	Volumetric flow rates for the lateral channels ( $\text{m}^3 \text{s}^{-1}$ )
$Q_f$	Volumetric flow rates of the focused stream ( $\text{m}^3 \text{s}^{-1}$ )
$R$	Radius of the particles (or molecules) (m)
$Re$	Reynolds number
$St$	Strouhal number
$t$	Time (s)
$T$	Absolute temperature
$u$	Velocity of fluid ( $\text{m s}^{-1}$ )
$v_2$	Average flow velocity of the flow within central inlet channel ( $\text{m s}^{-1}$ )
$v_f$	Average flow velocity of the flow within focused stream ( $\text{m s}^{-1}$ )
$v_o$	Average flow velocities of the flow within the mixing channel ( $\text{m s}^{-1}$ )
$w_2$	Width of central inlet channel (m)
$w_f$	Width of the focused stream (m)
$w_o$	Width of the mixing channel (m)
$x$	Position of the species (m)

## Greek Symbols

$\gamma$	Interfacial tension ( $\text{N m}^{-1}$ )
$\varphi$	Species concentration ( $\text{Kg m}^{-3}$ )
$\rho$	Fluid density ( $\text{kg m}^{-3}$ )
$\mu$	Fluid dynamic viscosity ( $\text{Pa s}$ )
$\nu$	Fluid kinematic viscosity ( $\text{m}^2 \text{s}^{-1}$ )

## Abbreviations

$\mu$ TAS	Micro total analysis systems
ASM	Asymmetric serpentine micromixer
CDM	Circulation–disturbance micromixer
CGM	Connected-groove micromixer
CMM	Crossing manifold micromixer
EKI	Electrokinetic instability
EWDO	Electrowetting on dielectrics
LOC	Lab on a chip
MHD	Magneto hydrodynamic
PCR	Polymerase chain reaction
PSM	Planar serpentine micromixer
SAR	Split-and-recombine micromixers, sequential lamination micromixers
SGM	Slanted-groove micromixer
SHM	Staggered-herringbone micromixers
SOC	Staggered overlapping crisscross micromixer

## 1 Introduction and Outline

Over the past two decades, lab-on-a-chip (LOC) technologies have driven considerable progress in the development of microsystems, particularly for chemical, biological, and medical applications. LOC technology has been applied in a wide range of processes such as nanoparticle crystallization [1, 2], extraction [3–5], polymerization [6–9], organic synthesis [10–12], enzyme assay [13, 14], protein folding [15], biological screening [16, 17], analytical assay [18–20], cell analysis [21, 22], bioprocess optimization [23, 24], clinical diagnostics [25, 26], and drug delivery studies [27].

The miniaturized systems, designed for the above cited applications, are generally implemented with a microscale mixer to provide an intimate contact between the reagent molecules for interactions/chemical reactions. Furthermore, beside their integration in more complex micro total analysis systems ( $\mu$ TAS) [28], microscale mixers could also work as stand-alone devices for applications where a superior control and a scaling-down of the mixing process are required.

The exponential increase of research in miniaturization and in microfluidic applications highlights the importance of understanding the theory and the mechanisms that govern mixing at the microscale level. This chapter will review the most recent research and developments in mixing processes within microfluidic devices. In order to better understand the rationale behind the design of the microfluidic mixers reported in the literature, Sect. 2 will discuss the unique physical characteristics and theory of the microfluidic environment and their implications in the context of mixing. Then, an up-to-date critical review of the different types and designs of micromixers will be provided in Sect. 3.

Owing to the increasing interest in “digital” or droplet-based microfluidics, the microfluidic generation of microdroplets, the associated active and passive mixing process, and the manipulation of micro-sized droplets in microfluidic devices will also be covered.

Finally, a section summarizing the general advantages of microfluidic mixers/reactors is presented. Although of high interest and importance, an in-depth review of microfluidic mixers in a diversity of microsystems for specific applications is not addressed since it falls out of the scope of this chapter. The reader is therefore directed to a number of excellent recent review articles on the specific subjects [9, 19, 29–36].

## 2 The Microfluidic Environment and Mixing Principles

In this section, we will summarize the basic theory of fluid flow and the implications of using microfluidic devices for mixing purpose. Generally, the same laws that describe the flow at a macroscale govern fluid flow in the microenvironment. However, miniaturization confers additional characteristics that can be leveraged to perform processes not possible at a macroscale. Microfluidic devices, indeed, are not merely a miniature version of their macroscale counterparts because many physical characteristics, such as surface area-to-volume ratio, surface tension and diffusion, do not simply scale linearly from large to small devices. Another important feature is the omnipresence of laminar flow conditions because in the microfluidic channel viscous forces dominate. These factors become significant at a microscale level, and their effects should be taken into account during the design and implementation of LOC devices.

In other words, it must be noted that, rather than design microfluidic mixer as just a scaled-down copy of a macroscale mixing device, they should be designed in ways that leverage the physical characteristic of the mixing in a confined space.

### 2.1 Reynolds Number and Diffusion

Fluid flow is generally categorized into two flow regimes: laminar and turbulent. Laminar flow is characterized by smooth and constant fluid motion, whereas turbulent flow is characterized by vortices and flow fluctuations. Physically, the two regimes differ in terms of the relative importance of viscous and inertial forces. The relative importance of these two types of forces for a given flow condition, or to what extent the fluid is laminar, is measured by the Reynolds number ( $Re$ ):

$$Re = \frac{\rho u D_h}{\mu} = \frac{u D_h}{\nu}, \quad (1)$$

where  $\rho$  and  $\mu$  are the fluid density and dynamic viscosity, respectively;  $\nu$  is the kinematic viscosity;  $u$  is the velocity of fluid and  $D_h$  is the hydraulic diameter of the

channel. The hydraulic diameter of the channel is a characteristic number that depends on the cross-sectional geometry of the channel, and is given by:

$$D_h = \frac{4A}{P_{\text{wet}}}, \quad (2)$$

where  $A$  and  $P_{\text{wet}}$  are the cross-sectional area and the wetted perimeter of the channel, respectively.

At low  $Re$ , the viscous effects dominate inertial effects and a completely laminar flow occurs. In the laminar flow system, fluid streams flow parallel to each other and the velocity at any location within the fluid stream is invariant with time when boundary conditions are constant. This implies that convective mass transfer occurs only in the direction of the fluid flow, and mixing can be achieved only by molecular diffusion [37]. By contrast, at high  $Re$  the opposite is true. The flow is dominated by inertial forces and characterized by a turbulent flow. In a turbulent flow, the fluid exhibits motion that is random in both space and time, and there are convective mass transports in all directions [38].

Between the definite regimes of laminar and turbulent flow there is a transitional  $Re$  range. The exact values of this number range are a function of many parameters, such as channel shape, surface roughness, and aspect ratio. The transition  $Re$  is generally expected to be in the range of 1,500 and 2,500 for most situations [39]. For microfluidic systems,  $Re$  are typically smaller than 100 and the flow is considered essentially laminar. This characteristic has a direct consequence on mixing within microfluidic devices.

In an environment where the fluid flow is restrictedly laminar, mixing is largely dominated by passive molecular diffusion and advection. Diffusion is defined as the process of spreading molecules from a region of higher concentration to one of lower concentration by Brownian motion, which results in a gradual mixing of material. Diffusion is described mathematically using Fick's law:

$$j = -D \frac{d\varphi}{dx}, \quad (3)$$

where  $\varphi$  is the species concentration,  $x$  is the position of the species, and  $D$  is the diffusion coefficient. For simple spherical particles,  $D$  can be derived by the Einstein–Stokes equation:

$$D = \frac{kT}{6\pi\mu R}, \quad (4)$$

where  $k$  is Boltzmann's constant,  $T$  is the absolute temperature,  $R$  is the radius of the particles (or molecules) and  $\mu$  is the viscosity of the medium. The diffusion coefficient for a small molecule in water at room temperature has the typical value of  $10^{-9} \text{ m}^2 \text{ s}^{-1}$  [40].

Diffusion is a nonlinear process in which the time  $t$  required for a species to diffuse scales quadratically with the distance  $x$  covered. A simple case of diffusion can be modeled in one dimension by the equation:

$$x^2 = 2Dt, \quad (5)$$

where  $t$  is the average time for particles to diffuse over the distance  $x$ . Regarding the microfluidic channel,  $x$  represents the stream width of the fluid to be mixed along the microfluidic channel [41]. On a microfluidic length scale, the diffusion distance can be extremely small, particularly if the fluid streams are hydrodynamically focused. Because  $x$  varies with the square power, a decrease in distance dramatically reduces the time required for complete mixing. Therefore, diffusion becomes a viable method to move particles and mix fluid in microfluidic devices.

## 2.2 *Mixing in Microfluidic Devices*

At a macroscale level, mixing is conventionally achieved by a turbulent flow, which makes possible the segregation of the fluid in small domains, thereby leading to an increase in the contact surface and decrease in the mixing path. As discussed in the previous section, the  $Re$  is small in microfluidic systems, implying that hydrodynamic instability does not develop; therefore, the flows cannot be turbulent. Owing to this limitation, mixing in microfluidic devices is generally achieved by taking advantage of the relevant small length, which dramatically increases the effect of diffusion and advection.

Micromixers are generally designed with channel geometries that decrease the mixing path and increase the contact surface area. According to the two different basic principles exploited to induce mixing at the microscale, micromixers are generally classified as being passive or active.

Active micromixers use external energy input as well as fluid pumping energy to introduced time-dependent perturbations that stir and perturb the fluid for accelerating the mixing process [42]. The type of external force employed by active micromixers can be further categorized as pressure field-driven [43], acoustic (ultrasonic)-driven [44], temperature-induced [45] or magneto-hydrodynamic [46]. Generally, active micromixers have higher mixer efficiency [47]. However, the requirement to integrate peripheral devices such as the actuators for the external power source into the microdevice, and the complex and expensive fabrication process, limit the implementation of such devices in practical applications. In addition, in active mixing mechanisms such as ultrasonic waves, high temperature gradients can damage biological fluids. Therefore, active mixers are not a popular choice when applying microfluidics to chemical and biological applications [48].

Passive mixing devices rely entirely on fluid pumping energy and use special channel designs to restructure the flow in a way that reduces the diffusion length and maximizes the contact surface area. Passive mixers were the first microfluidic device reported, often entail less expense and more convenient fabrication than active micromixers, and can be easily integrated into more complex LOC devices. The reduction in mixing time is generally achieved by splitting the fluid stream

using serial or parallel lamination [49, 50], hydrodynamically focusing mixing streams [51], introducing bubbles of gas (slug) or liquid (droplet) into the flow [52, 53], or enhancing chaotic advection using ribs and grooves designed on the channel walls [54, 55].

Micromixers are also commonly characterized accordingly to three nondimensional fluid parameters:  $Re$  (as discussed above), Peclet number  $Pe$ , and Strouhal number  $St$ . Peclet number is defined as:

$$Pe = \frac{uL}{D}, \quad (6)$$

which is a measure of the relative importance of advection and diffusion in providing the mass transport associated with the mixing. Advection is dominant at high  $Pe$ .

The Strouhal number is defined as:

$$St = \frac{fD_h}{u}, \quad (7)$$

where  $f$  is the frequency of the disturbance action, is generally associated with active micromixers, and represents the ratio between the residence time of a species and the time period of disturbance [48, 56, 57].

### 3 Micromixers

#### 3.1 Passive Micromixers

Passive micromixers rely on the mass transport phenomena provided by molecular diffusion and chaotic advection. These devices are designed with a channel geometry that increases the surface area between the different fluids and decreases the diffusion path. By contrast, the enhancement of chaotic advection can be realized by modifying the design to allow the manipulation of the laminar flow inside the channels. The modified flow pattern is characterized by a shorter diffusion path that improves the mixing velocity. In this section, an overview of the different types of passive micromixers is provided. Mixed phase passive micromixers can be categorized as:

1. T- and Y-shaped micromixers
2. Parallel lamination micromixers
3. Sequential lamination micromixers
4. Focusing enhanced mixers
5. Chaotic advection micromixers
6. Droplet micromixers

### 3.1.1 T- or Y-Shaped Micromixers

The easiest and most basic design for a micromixer is represented by either T- or Y-shaped channel micromixers [58–61]. A schematic of the general design of this type of mixer is shown in Fig. 1.

The mixing process in this type of micromixer is obtained by guiding the two liquids to be mixed in contact through a flow-through channel. It must be noted that, for the basic design of T- and Y-type micromixers, mixing solely depends on diffusion of the species at the interface between the two liquids, hence the mixing is rather slow and a long mixing channel is required. In order to enhance the mixing efficiency, different authors proposed slight modifications to the geometrical setup by adding obstacles or roughening the channel walls [54, 59, 62]. Further reduction of the mixing time could be achieved by using a high flow rate, hence high  $Re$ , where a chaotic flow is expected [63, 64], (Fig. 2). Veenstra et al. further reduced the mixing path in a T-shaped micromixer by a simple narrowing of the mixing channel and therefore shortening of the diffusion length [65].

### 3.1.2 Parallel Lamination

The concept of T- and Y-shaped micromixers can be improved by using more complicated designs that split the inlet main streams into  $n$  sub-streams and then rejoin them to form a laminate stream (Fig. 3) [66, 70–72]. This type of micromixer enhances the mixing process by decreasing the diffusion length and increasing the contact surface area between the two fluids.

According to Erbacher et al., the subdivision of each stream into  $n$  laminae leads to mixing that is faster by a factor of  $n^2$ , as reported in the following expression derived from (5) [66]:

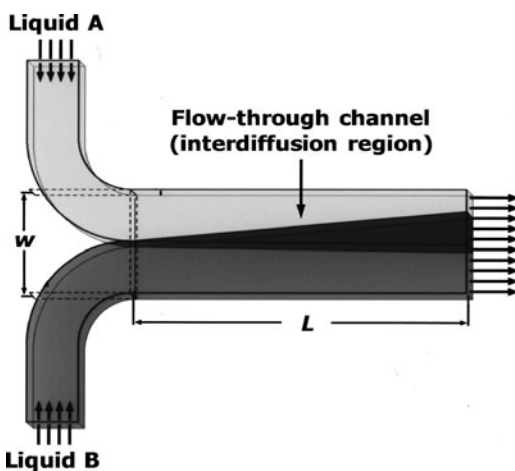


**Fig. 1** T-shaped micromixer with two input fluids, each containing one diffusing species.  $L$  and  $w$  represent the length and width of the mixing channel, respectively (Adapted with permission from [58]. Copyright 1999 American Chemical Society)



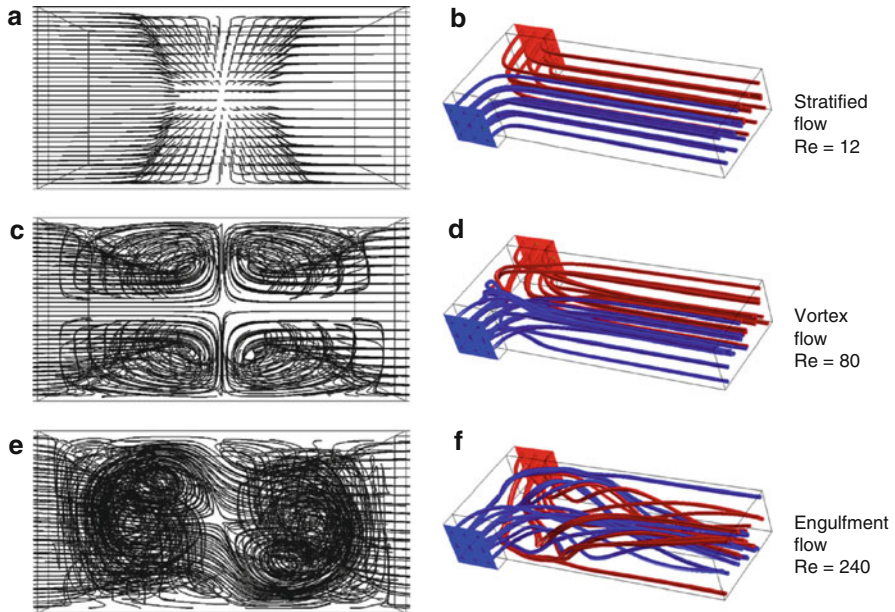


**Fig. 2** Path lines (a, c, e) and streamlines (b, d, f) for different  $Re$  numbers of 12 (a, b), 80 (c, d) and 240 (e, f). The swirling of the fluid flow obtained at higher  $Re$  number results in better dispersion of the fluid within the channel volume and hence an improvement in the mixing quality (Reprinted from [61]. Copyright (2008) with permission from Elsevier)

$$t = \frac{x^2}{2n^2D}, \quad (8)$$

where  $n$  is the number of parallel fluid substreams.

Lamination of the fluids to be mixed can be achieved using two different feeds arrangements known as (1) bifurcation-type feeds and (2) parallel interdigital-type feeds. Bifurcation-type feeds [66, 70–72] are characterized by an alternate arrangement of feeds (Fig. 3a) that are later joined by passing through an inverse bifurcation channel pattern followed by a folded mixing channel in which the mixing takes place. By exploiting this configuration, Bessoth et al. [70] demonstrated that mixing was completed is less than 100 ms, while 95% of mixing was achieved in 40 ms.

Parallel-flow interdigital-type feeds is the most-used feeding concept. This type of micromixer comprises a feeding structure characterized by a co-[67, 73–76] or counterflow [77] interdigital array of microchannels. Similar to the previous types of feed concept, the microchannel array leads to an alternate lamellae arrangement of the liquid to be mixed. However, unlike bifurcation-type feeds, the way to obtain this pattern is based on a pressure-loss triggered flow equipartition (Fig. 3b). Generally, after the lamellae rearrangement, the multilaminated flow is focused through a geometrical constrain (mixing channel narrowing) [67, 71, 73, 75, 76] in

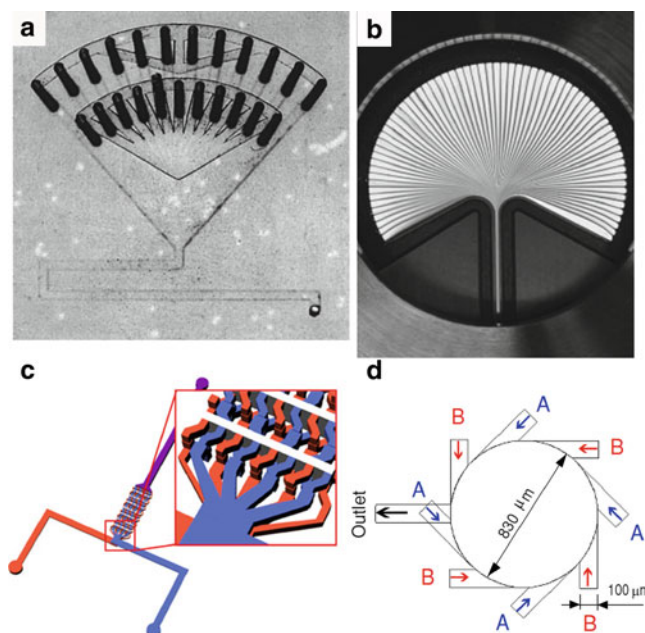


**Fig. 3** Parallel lamination micromixer types: (a) Bifurcation-type feeds (Adapted from [66] with kind permission from Springer Science). (b) Interdigital-type feeds, super focus mixer (Reproduced from [67] with permission. Copyright Wiley-VCH ). (c) Chessboard micromixer (Adapted from [68] with permission. Copyright IOP Publishing). (d) Circular micromixer (Adapted from [69] with permission. Copyright IOP Publishing)

order to decrease the diffusion length and enhance the mixing, using a concept similar to that presented by Veenstra et al. [65] for a T-type micromixer.

Drese et al. [73], developed a special interdigital-type feed micromixer, named the super focus mixer (Fig. 3b), in which the various lamellae have a different angle with respect to the channel direction and which is capable of obtaining 95% mixing in 4 ms.

Interdigital-type feed micromixers were recently applied as a reactor for a nitroxide-mediated radical polymerization, demonstrating a control over the molecular weight distributions as a result of an improved control of the co-polymerization reaction [78, 79].

Cha et al. [68] presented a novel micromixer design relying on a concept not far from that of the multilamination mixer, named a chessboard mixer. The mixer was able to complete the mixing in only 1.400 mm and the author claimed that the flow rate can be increased easily by using different arrays without affecting the performance (Fig. 3c).

A further interesting concept for the creation of multilaminated streams is that applied in circular micromixers [69, 80, 81]. Circular micromixers rely on the formation of a vortex due to the self-rotation of the fluid stream injected in a quasitangential orientation to the circular mixing chamber (Fig. 3d). Excellent

mixing performance of this type of micromixer was reported at either high ( $Re = 150$ ) [80] or low [81]  $Re$  number ( $Re = 4$ ).

Lastly, StarLaminators are devices based on a multilamination concept and are capable of high liquid throughput up to  $1,000 \text{ Lh}^{-1}$  [56, 82, 83]. The mixing is provided by a stack of plates with star-like openings that leads to turbulent flow, which causes mixing by formation of eddies.

### 3.1.3 Sequential Lamination

Similar to parallel lamination micromixers, sequential lamination micromixers [also called split-and-recombine (SAR) micromixers] rely on an exponential increase in the contact surface area and decrease in the length path to achieve a shorter mixing time. The difference between the two types of micromixers is the method used to achieve lamination of the fluid to be mixed. As suggested by the name, the lamination in sequential lamination micromixers is obtained by sequential processes of splitting and rejoining the fluids (Fig. 4a) [84, 86–89].

Different geometries for SAR micromixers have been proposed, such as ramp-like [86] and curved-like [90] architectures. However, in order to achieve exponential sequential lamination, three steps are typically required: flow splitting, flow recombination, and flow rearrangement (Fig. 4a).

It must be noted that SAR mixers generally work at small  $Re$ . However, some secondary recirculation flows can be generated, as demonstrated by particle tracking simulation [90].

Recently, Fang et al. [85] proposed a SAR micromixer incorporating chaotic advection features named (SAR  $\mu$ -reactor design) to mix fluids in a wide range of  $Re$  and viscosity (Fig. 4b–c). They compared the results with those obtained from a slanted-groove micromixer (SGM) (see Sect 3.1.5) [55], demonstrating better mixing efficiency of the SAR  $\mu$ -reactor compared to SGM as result of the synergistic effect of the two mixing concepts.

Bertsch et al. [91] presented two micromixers, similar in concept to the SAR micromixer, with internal structures resembling conventional large-scale static mixers (Fig. 5). The first micromixer was characterized by introducing an internal structure with intersecting channels, which worked in a similar way to a SAR micromixer by splitting and recombining fluid streams. The second micromixer comprised a series of helical elements (Fig. 5a). Computational fluid dynamics (CFD) simulated results showed the higher mixing efficiency of the first type of micromixer over a helical based mixer.

Recently Lim et al. [92] presented a three-dimensionally micro-mixer, named crossing manifold micromixer (Fig. 5b). The micromixer was able to perform almost complete mixing of 90% channel length of  $250 \mu\text{m}$ .

The main disadvantage of SAR mixers is the complex fabrication process required to make a 3D structure. However, an effect on the liquid stream similar to that exploited by SAR can be achieved by a planar, packed bed configuration that enhances trans-channel coupling. Melin et al. [93] fabricated and tested multiple

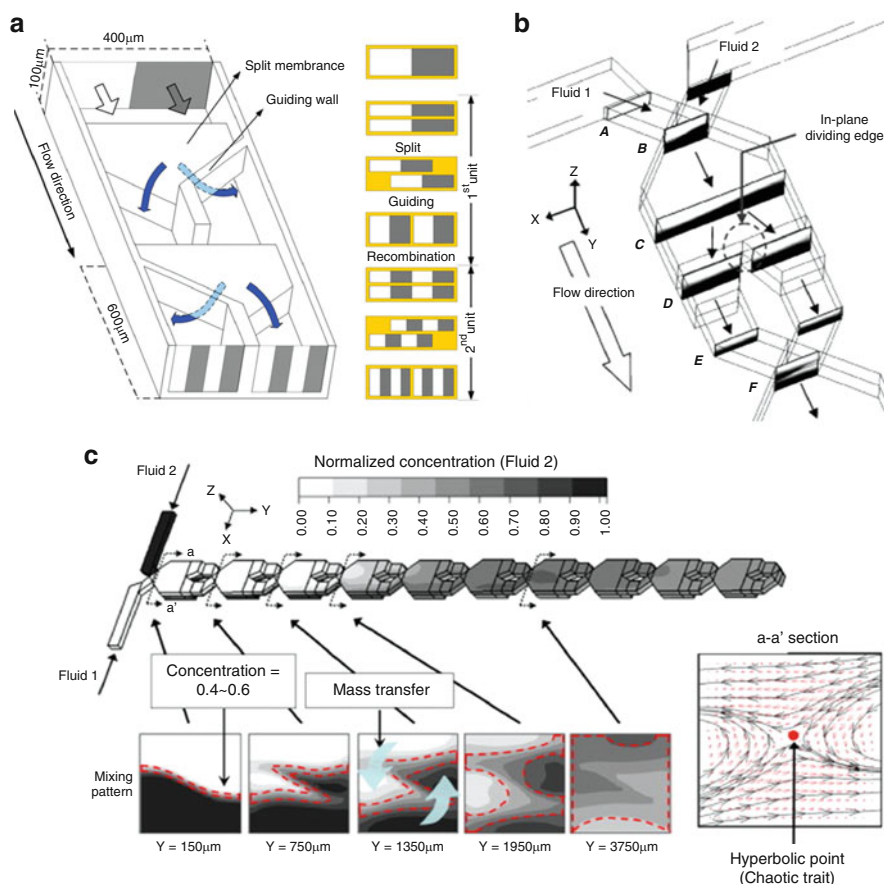


**Fig. 4** Sequential lamination micromixer (I): (a) Mixing unit of the SAR micromixer and corresponding cross-section view of the laminated flow (Adapted from [84] with permission. Copyright IOP Publishing). (b) Mixing unit and (c) computed cross-section view of fluid arrangements along the SAR  $\mu$ -reactor ( $Re = 1$ ). Chaotic advection generated by the fluids overlapping causes the fluid interface to rotate, increasing the mixing efficiency (Reprinted from [85] with permission. Copyright 2009 Elsevier)

intersecting microchannels (known as a packed bed micromixer) that create a constantly changing flow pattern as the liquid samples pass through the mixing chamber, and achieved homogenous mixing of the two fluids in just 0.4 s. This concept was also applied to electrokinetically driven flow, as reported by He et al. [94] (Fig. 6a).

Another way of obtaining a SAR-like effect within a planar microfluidic chip was introduced by Sudarsan et al. [95] (Fig. 6b). It works with a multistep action: Initially, this geometry leveraged the generation of Dean vortices that arise in the vertical plane of curved channels to induce a  $90^\circ$  rotations in the fluid. At this point, the fluid is

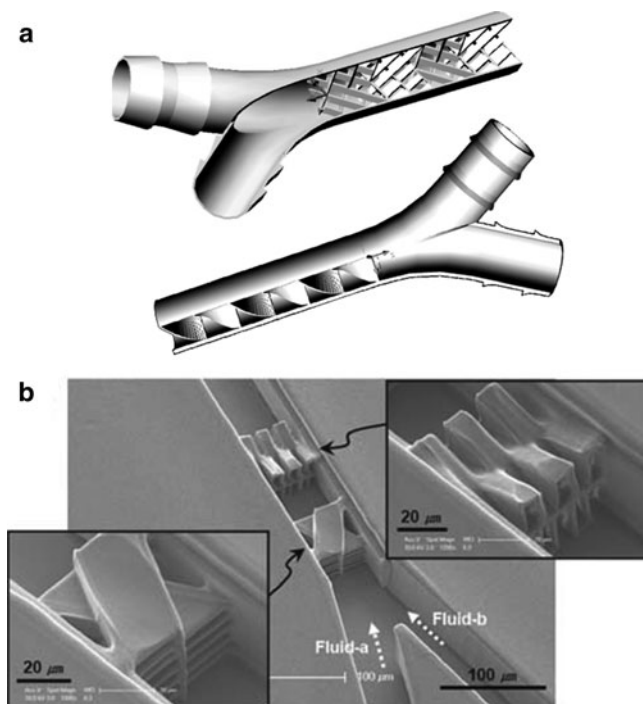


**Fig. 5** Sequential lamination micromixer (II): (a) Static micromixer, with intersecting channel (*top*) and helical elements (*bottom*) (Reproduced from [91] by permission of The Royal Society of Chemistry). (b) Internal structure of crossing manifold micromixer (CMM) (Reproduced from [92] by permission of The Royal Society of Chemistry)

divided into many substreams that undergo the same  $90^\circ$  rotations in the fluid. At the end, the transformed substreams rejoin to create a multilamellae arrangement.

### 3.1.4 Flow Focusing

Another solution for reducing the mixing path is hydrodynamic focusing [51]. The basic design for hydrodynamic focusing is a long microchannel with three inlets (Fig. 7).

In hydrodynamic focusing, a central sample solution (supplied from the middle inlet) flows within the sheath of outer fluids (supplied from the side inlets), which constrain laterally the inner sample flow to achieve a smaller stream and thinner lamination width. The extent of the width decrease of the focused stream depends on the volumetric flow rate ratio between the sample flow and sheath flows. The greater the flow rate difference, the greater the degree of width reduction. As indicated by (5), mixing time is inversely proportional to the square of the diffusion path length (in this case represented by the focused stream width), therefore,

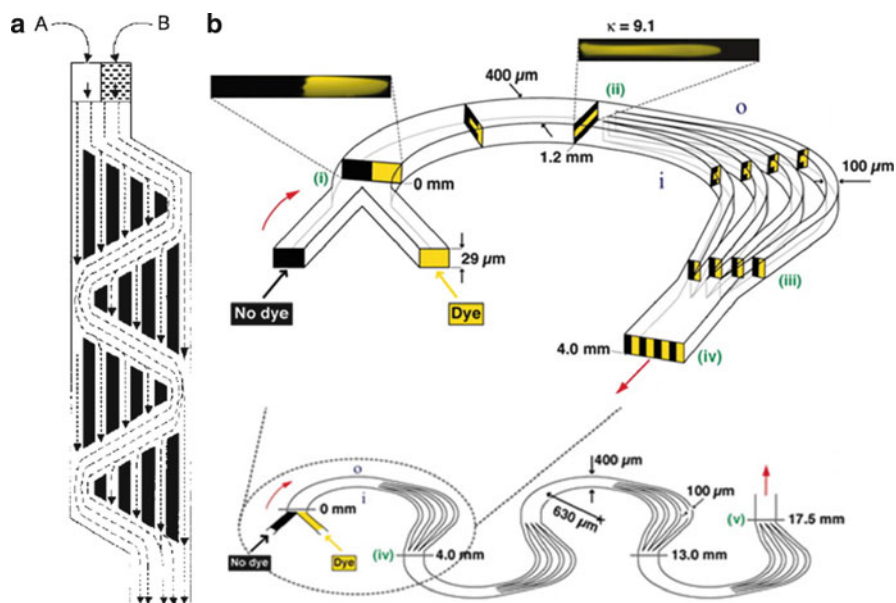


**Fig. 6** Planar SAR-like micromixers: (a) Mixing unit of a packed bed micromixer (Adapted from [94] with permission. Copyright 2001 American Chemical Society). (b) Planar SAR micromixer that relies on Dean flows to generate alternate lamellae of fluid in a SAR-like fashion (Adapted from [95] with permission. Copyright 2006 National Academy of Sciences, USA)

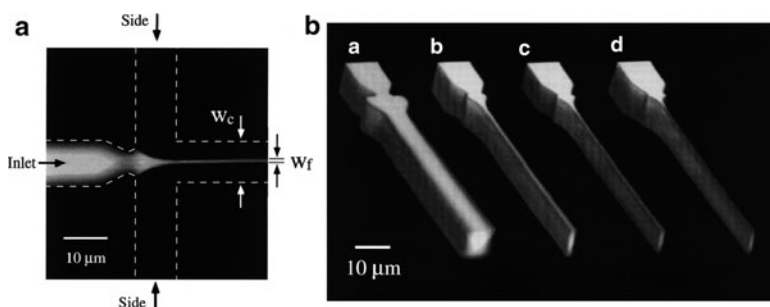


**Fig. 7** (a) Focusing enhanced mixer. (b) Effect of ratio  $\alpha$  of the side pressure to the inlet pressure on the width of the focused stream: (a) 0.5, (b) 1.0, (c) 1.1, and (d) 1.2 (Reprinted from [51] with permission. Copyright 1998 American Physical Society)

decreasing the stream width results in faster mixing. Notably, the position of the focused stream is also a function of the relative flow rate ratio of the three inlets. As a result, by changing the relative flow rate of the two side streams it is possible to direct the focused stream into a specific outlet [96].

The relative flow rate of the three streams is generally controlled using multiple external pressure sources or pumps (e.g., syringe pumps) (Fig. 7b). However, Stiles



et al. proposed and tested the use of a vacuum-pumped microfluidic device using either a single suction pump or a capillary pumping effect to control the relative flow rates by varying the flow resistance of the input channels [97]. The analysis and prediction of the focused stream width employs a simple model based on mass conservation principles [98, 99]. The 2D focused stream width is computed under these simplified assumptions:

1. Flow in the microchannel is steady and laminar
2. Fluids are Newtonian
3. Fluids have the same density in the four channels (three inlet channels and one outlet channel)
4. Fluids flow in a rectangular microchannel
5. The four channels have the same height

According to the mass conservation principle, the volume of sample liquid that passes through the inlet channel ( $Q_2$ ) must match the volume of the focused stream:

$$Q_2 = v_2 w_2 h = v_f w_f h = Q_f. \quad (9)$$

This leads to (10):

$$w_f = \frac{Q_2}{v_f h}, \quad (10)$$

In (9) and (10),  $w_f$  and  $w_2$  represent the width of the focused stream and central inlet channel, respectively.  $Q_2$  and  $Q_f$  are the volumetric flow rates of the central inlet channel and focused stream, respectively.  $h$  is the height of the channels, and  $v_2$  and  $v_f$  are the average velocity of the flow in the central inlet channel and of the focused stream, respectively. The amount of fluid passing through the outlet channel (channel O) must be equal to the total amount of the fluid supplied from the three inlets:

$$Q_o = w_o v_o h = Q_1 + Q_2 + Q_3, \quad (11)$$

$$w_o = \frac{Q_1 + Q_2 + Q_3}{v_o h}, \quad (12)$$

where  $Q_1$  and  $Q_3$  are the volumetric flow rates for the two lateral channels, and  $v_o$  and  $w_o$  are the average velocities of the flow and width of the mixing channel, respectively. Combining (9) and (12), and assuming  $v_o$  and  $v_f$  have the same values, it is possible to obtain the relationship between the width of the focused stream and volumetric flow rate of the inlets:

$$\frac{w_f}{w_o} = \frac{Q_2}{Q_1 + Q_2 + Q_3}. \quad (13)$$

This equation provides a simple guideline for predicting the focused stream width. However, it does not reflect the effect of other factors such as device

structure, channel surface, and fluidic property, which could affect the focusing process. In this respect, Lee et al. [99] proposed a similar model in which the effect of the density of the different fluids is taken into account. Moreover, Wu and Nguyen [100] presented a more complex method that considered the effect of the different viscosities of the sample stream and sheath streams.

In recent years, more complex channel geometry structures that rely on the hydrodynamic focusing to achieve mixing have been fabricated and examined. Wu and Nguyen [101] reported a mixer with two sample streams (solvent and solute streams). The two streams are brought into contact and then focused by two lateral sheath streams. The dramatic decrease in the diffusion path length improves mixing significantly. Park et al. [102] described a novel five-inlet port mixer in which the additional two diagonal sheath flows served as a barrier between solutions flowing from the center and the two side channels during the focusing process. In that configuration, the additional sheath reduced premixing before the formation of the focused jet without compromising rapid mixing by diffusion. Nguyen and Huang [103] reported a microfluidic mixer that relied on a combination of hydrodynamic focusing and sequential segmentation to reduce the mixing path and shorten mixing times. The sequential segmentation step divided the solvent and the solute into segments that usually occupied the whole channel width. Because of the additional segmentation step, the dispersion occurred even along the flow direction, leading to increased mixing efficiency.

Typically, focusing-enhanced micromixers focus the sample flow only in the horizontal dimension. Different authors have proposed microfabricated devices capable of focusing the sample horizontally and vertically [104–107]. Such devices add an additional dimension of focusing and are often referred to as 3D hydrodynamic focusing devices to distinguish them from traditional 2D focusing devices. Building these devices requires complex methods such as multistep photolithography, leading to an increase in fabrication cost. Recently, a novel fluid manipulation technique called “microfluidic drifting” was applied to obtain 3D focusing with a single-layer planar chip that is relatively easy to make [38, 108, 109] (Fig. 8).

The process of 3D focusing in this device can be divided into two steps. First, the sample stream is focused in the vertical direction using microfluidic drifting. The lateral drift of the sample flow is caused by the effect of the Dean vortices induced by the centrifugal effect of the curve, which transports the fluid in the opposite side of the channel. Second, classic horizontal focusing is obtained using two horizontal sheath streams. The result of these two steps is a stream focused in both the vertical and horizontal directions.

### 3.1.5 Chaotic Advection Micromixers

Advection is the transport of a substance within a moving fluid. In the micromixers discussed above, advection generally occurs in the direction of the flow, hence it has no effect on the transversal transport of the substance. However, advection in other directions, so-called chaotic advection [110], can generate a transverse



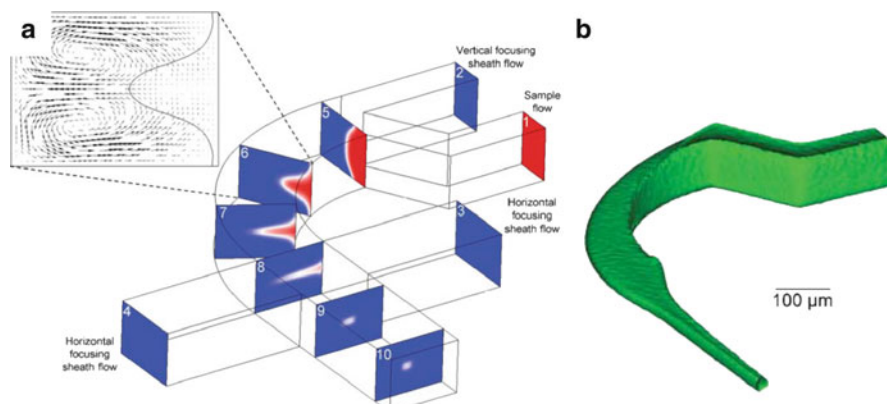


**Fig. 8** The “microfluidic drifting” process. (a) Slices 1–10 are the cross-sectional profiles of the sample stream in the device; *inset* shows formation of Dean vortices in the 90° curve. (b) 3D microfluidic drifting focusing characterized by confocal microscopy (Reproduced from [109] by permission of The Royal Society of Chemistry)

component of flow [55]. These generated transverse flow components cause an exponential growth of the interfacial area and a corresponding decrease in the striation thickness, which can significantly improve mixing.

These “stirring” transverse flows can be generated by channel shapes that stretch, fold, break, and split the laminar flow over the cross-section of the channel. This effect can be achieved using 2D curved [111–113], or 3D convoluted channels [114–116] and by inserting obstacles [117] and bas-reliefs on the channel walls [54, 118, 119]. It must be noted that such type of chaotic flow could also be achieved by an active mixing strategy such as one using electrokinetic instability (EKI), as described in Sect. 3.2.2.

The simplest way to induce transverse flow is to insert an obstacle into the mixing channel. Obstacles can be inserted into the walls of the microchannel [62] or into the channel itself [117, 120–122]. The presence of obstacles alters the flow direction, and the streamlines induce whirl flow and recirculation that create the transversal mass transport. Generally obstacles in microchannel are not very efficient in creating transverse flow unless they are used at moderately high  $Re$  (typically more than 100) [120]. However, Bhagat et al. [121, 122] recently reported a micromixer with optimized cubic and rectangular structure capable of mixing with  $Re < 1$  (Fig. 9).

Another efficient solution to induce transverse flows and chaotic advection at small  $Re$  (typically  $Re \approx 1$ ) is to use a channel wall with a grooved pattern. SGM [55, 118] and staggered-herringbone micromixers (SHM) [55] subject the fluid to a repeated sequence of rotational and extensional local flow that, as result, produces a chaotic flow. The internal structures endow SHM with high mixing efficiency compared to the classic T-type mixer without them. In particular, a classic T-shaped mixer requires a mixing length (1–10 m) that is two order of magnitude larger than SHM mixers (1–1.5 cm) at  $Pe$  within  $10^{-4}$  to  $10^{-5}$ .

A series of improved grooved pattern micromixers has been proposed. A modified SHM micromixer that utilizes sequences of asymmetrical herringbone grooves

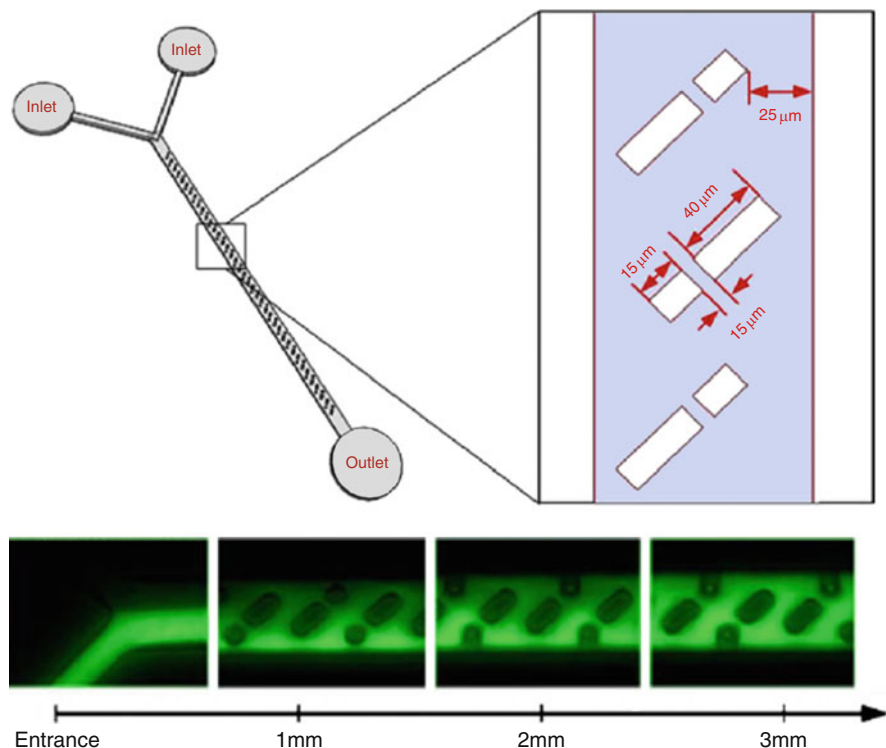


**Fig. 9** Mixer with rectangular structure and *inset* reporting key features and dimension (*above*). Mixing extent at various portions downstream of the entrance at  $Re = 0.05$  (*below*) (Adapted from [121] with permission. Copyright IOP Publishing)

was introduced and computationally studied by Hassel et al. [119]. Different authors have proposed micromixers in which the grooved pattern and zigzag barriers are not only applied on the bottom wall of the channel but also on the side and top walls to promote mixing, named respectively connected-groove micromixer (CGM) [123] (Fig. 10a) and circulation–disturbance micromixer (CDM) [124, 125] (Fig. 10b). Adding additional mixing elements to the side and top walls promotes lateral mass transport and assists the formation of advection patterns increasing mixing efficiency. In particular, CGM showed a mixing performance over 50% better than the classic SGM for  $Re$  ranging from 1 to 100 as a result of the intense transverse transport induced in the fluids [123].

Chaotic advection can be induced with a 2D alternatively curved microchannel (2D serpentine) [112, 113] or zigzag channel shape [111]. In the first case, the chaotic advection is induced in the curved microchannel by consecutive generation of Dean vortices (Fig. 11a). Typically such type of micromixer can provide an effective mixing only for high  $Re$  in the range of few hundreds. These micromixers are generally described using another dimensionless number, the Dean number ( $De$ ):

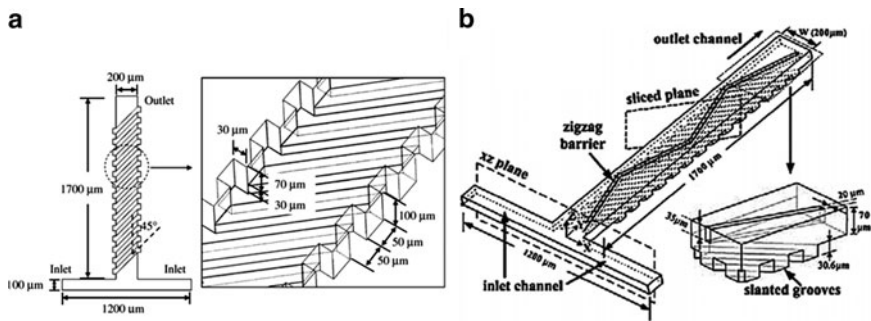


**Fig. 10** Micromixers with grooved pattern: (a) Connected-groove micromixer (CGM) and inset reporting key features and dimension (Reprinted from [123] with permission from Elsevier. Copyright 2008). (b) Schematic representation of circulation-disturbance micromixer (CDM) and inset reporting key features and dimension (Adapted from [124] with permission. Copyright IOP Publishing)

$$De = Re \sqrt{\frac{D_h}{R}} \quad (14)$$

where  $R$  represent the channel curvature. Jiang et al. [112] demonstrated that in order to provide an efficient mixing  $De$  must be greater than 140.

Sundarsan et al. [95, 127] reported two improved 2D serpentine micromixers, namely the planar spiral micromixer [127] and the asymmetric serpentine micromixer (ASM) [95] (Fig. 11a). Both the micromixers were able to produce effective mixing at low  $Re$  number. The mixing enhancement was due to the synergistic effect of Dean and expansion vortices, where the latter were introduced by abrupt expansions of the microchannels.

In a zig-zag micromixer [111], mixing is provided by laminar recirculation that induces trasverse velocity components localized at each channel angle. The micromixer studied had a critical  $Re$  number ( $Re = 80$ ), below which the mixing was solely due to molecular diffusion (see Fig. 11c).

Another interesting planar structure able to induce chaotic advection has been reported by Hong et al. [126] (Fig. 11d). This micromixer comprised a modified tesla structure that redirected the streams, by exploiting the Coanda effect. The authors demonstrated an efficient mixing at relative low  $Re$  number ( $Re < 10$ ).

Based on the 2D twisted micromixers, the so-called 3D serpentine micromixers (or 3D twisted micromixers) have been developed. These micromixers have a complex 3D structure with a repetition mixing unit that induces the formation of secondary flows that stretch and fold the fluids. Different channel arrangements have been presented. Liu et al. [115] fabricated a 3D structure created by a series of C-shaped segments aligned in a perpendicular plane. The authors showed that the microreactor performed well at relatively high  $Re$  number, ( $Re > 25$ ) and that the mixing efficiency increased with an increase of the  $Re$  number. A 3D structure comprising an L-shaped segment aligned in the perpendicular plane has also been presented (Fig. 12) [116].

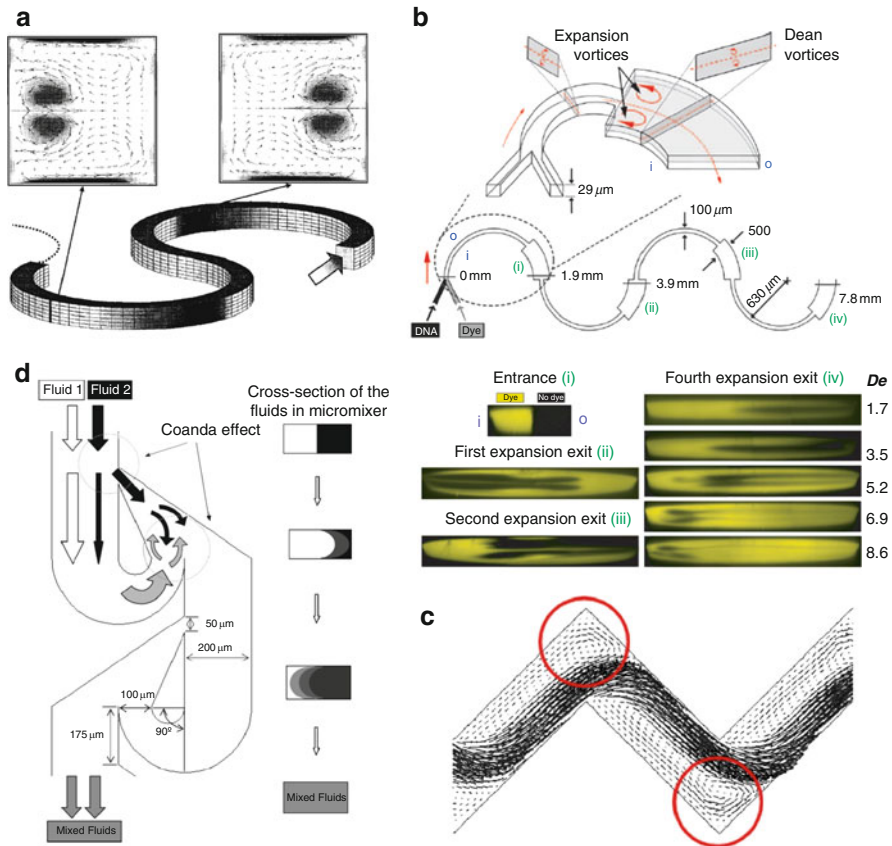


**Fig. 11** Planar micromixer for chaotic advection: (a) 2D serpentine micromixer and *insets* showing the cross-section view of the channel and corresponding secondary Dean flows vortices (Adapted from [113] with permission. Copyright 2004 American Institute of Chemical Engineers ). (b) Asymmetric serpentine micromixer (ASM) (*top*) and confocal cross section view showing synergistic effect of Dean vortices and expansion vortices at different section along the mixer and at different  $De$  number (Adapted from [95] with permission. Copyright 2006 National Academy of Sciences, USA). (c) Zigzag micromixer and recirculating pattern created at each zigzag (Adapted from [111] with permission). (d) Mixer with modified tesla structure and their effect on the liquid interface (Adapted from [126] with permission. Copyright 2002 American Chemical Society)

Chen et al. [114] reported a more complex structure derived from the connection of two helical flow channels with opposite chirality, and called it a topological mixer. By splitting, rotating and recombining the flow streams, the micromixer provided an effective and fast mixing at low  $Re$  between 0.1 and 2.

Park et al. [128] reported a structure that added the break-up effect in order to increase mixing efficiency. The break-up process enhances the mixing process by increasing the interfacial area as a result of the production of smaller fragments of blobs. Another interesting approach using a 3D structure was recently developed by

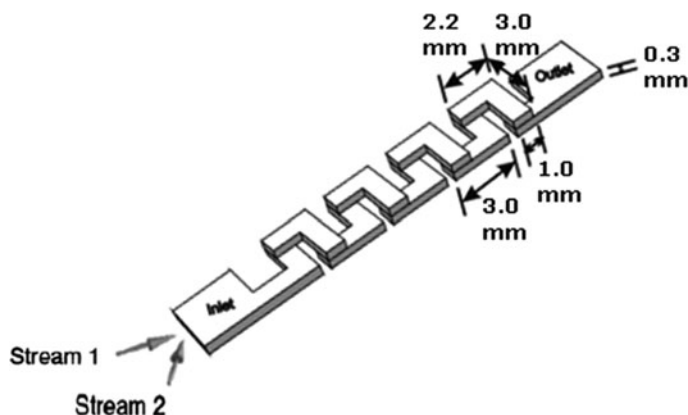


**Fig. 12** 3D serpentine micromixers with L-shaped segment. (Adapted from [116] with permission. Copyright 2003 American Chemical Society)

Long et al. [129]. They used an easily fabricated 3D structure comprising a circular chamber in which inlet and outlet channel are connect tangentially. When the two liquids to be mixed flow in the circular chamber, a vortical motion is generated. The vertical motion provides distortions and elongations of material interfaces and high mixing efficiency at relatively low  $Re$  ( $Re > 21$ ).

Also, many micromixers combining chaotic advection and an SAR approach have been presented [85, 130–133]. Park et al. [130] and Kim et al. [131] presented a serpentine-laminating micromixer (Fig. 13a, b). These micromixers have a series of F-shaped mixing units that combine the effect of a 3D serpentine structure with a splitting/recombination mechanism. Wang et al. [132, 133] reported a micromixer that combines the effects of a grooved surface and a splitting/recombination process (Fig. 13c, d). This micromixer, called staggered overlapping crisscross micromixer (SOC  $\mu$ -mixer), consists of an overlapping crisscross entrance and asymmetrical herringbone grooved surface channels. The author demonstrate 46% better mixing indices at the same longitudinal distance when compared with the SHM mixer. The authors claimed that the superior mixing characteristic was due to the induction of vertical tumbling near the intersections of the two crossing channels.

### 3.1.6 Multiphase Microfluidics and Microdroplet-Based Mixers

Microdroplets can be generated within microfluidic devices using different methods such as electric fields [134], micro-injectors [135] and needles [136]. However, the most widely used methods for droplet generation rely on flow instabilities between immiscible fluids that lead to the so-called multiphase flow. Any fluid flow consisting of more than one phase or component (e.g., emulsions and foams) are examples of multiphase fluids. Traditional emulsification methods are based on the agitation of immiscible fluids and result in the formation of a polydisperse collection of droplets. By

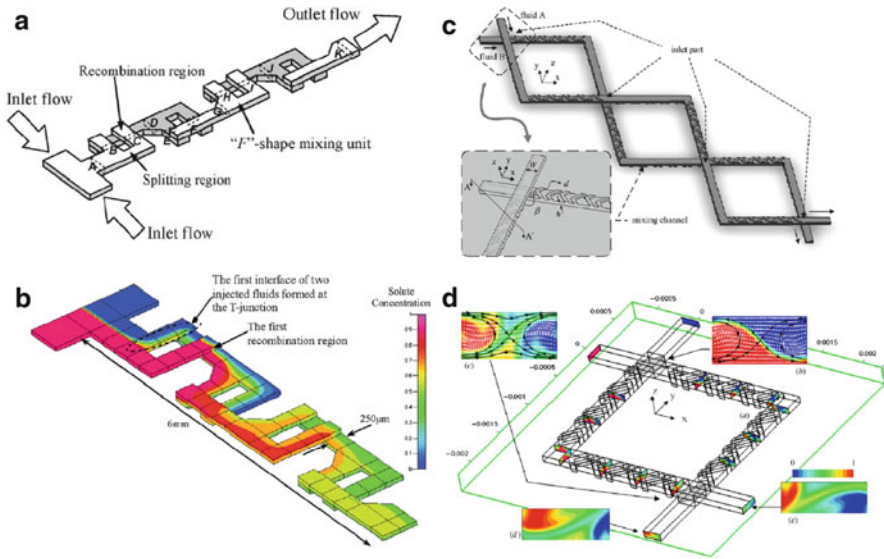


**Fig. 13** Micromixer combining SAR and chaotic advection approaches: **(a)** Serpentine laminating micromixer (SLM) and **(b)** concentration contours along the mixers channels, (Reproduced from [131] by permission of The Royal Society of Chemistry). **(c)** Staggered overlapping crisscross micromixer (SOC  $\mu$ -mixer) and **(d)** corresponding cross-section view showing concentration profiles after flowing through two junctions (Adapted from [132] with permission. Copyright IOP Publishing)

contrast, methods based on the use of microfluidic devices have been shown to produce highly monodisperse emulsions with a small size variation (e.g.,  $<1\%$ ) [53, 137–140].

In microfluidic devices, multiphase flows are created when two (or more) immiscible fluids come into contact. Depending on the interaction between the interfacial and viscous forces, the resulting multiphase flow can take different forms, such as suspended droplets, slugs (droplets occupying the whole channel) or stratified flow (parallel) [141, 142]. In addition to the forces exerted between the two liquids, the channel geometry and physical characteristics also play an important role in the process [143]. In this respect, the use of hydrophobic channels is suitable for the formation of water-in-oil emulsions, whereas hydrophilic channels favor the creation of oil-in-water emulsions [144].

Capillary number ( $Ca$ ) is a parameter that expresses the competition between viscous and interfacial forces, and is generally used to describe multiphase flow behavior in micro- and nanochannels.  $Ca$  is defined as the ratio between the viscous and interfacial force:

$$Ca = \frac{\mu u}{\gamma}, \quad (15)$$

where  $\mu$  is the viscosity of the continuous phase,  $u$  is the average flow velocity, and  $\gamma$  is the interfacial tension between the two fluid phases. The viscous forces mainly act tangentially to the fluid interface causing the elongation of it, whereas the



interfacial force acts preferentially normal to the interface and leads to droplet or slug formation [145]. Generally, when viscous forces dominate interfacial forces, a stratified flow occurs, whereas capillary instability leads to the formation of segmented flow when the interfacial forces dominate.

The basic channel configurations used to generate multiphase flows include the T-junction and flow focusing configurations (Fig. 14a, b). In the T-junction configuration, the channel transporting the dispersed phase intersects perpendicularly with the continuous phase channel, and an emerging droplet is formed at the intersection of the two channels. The effect of the viscous force generated by the continuous phase flow, and the pressure gradient generated upstream of the junction, causes the narrowing of the neck and merging of the droplet, which eventually breaks, leaving the liquid plug (or droplet) flowing downstream. By varying the viscosity of the two phases, the relative flow rates, or the channel dimension it is possible to tune the dimensions of the produced microdroplets [146, 148, 149].

In flow focusing configuration (Fig. 14c, d), the dispersed phase flows in the middle channel, whereas the continuous phase flows in two lateral channels [147,

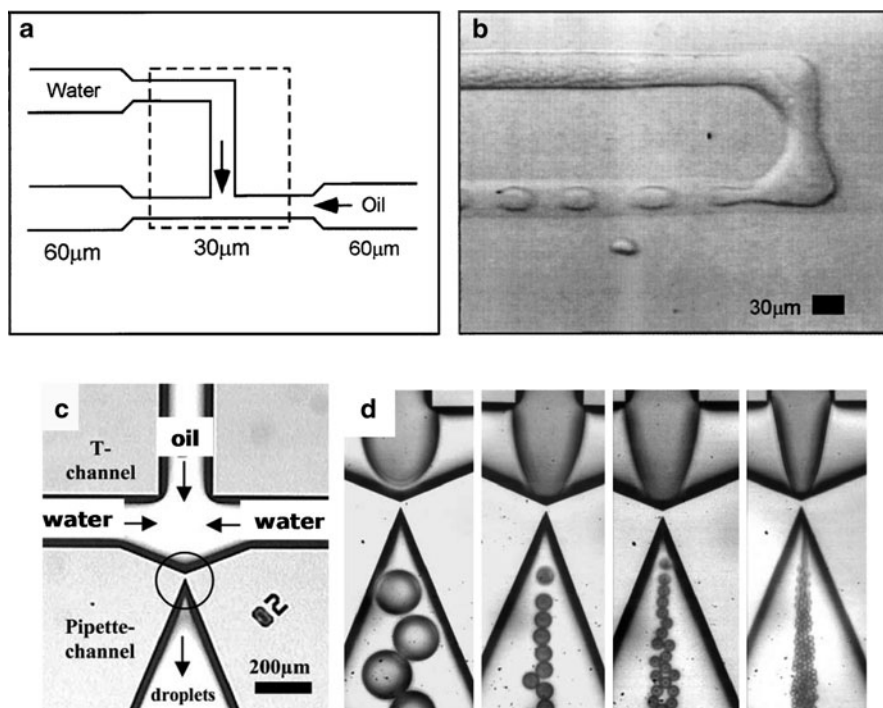


**Fig. 14** Mechanism of droplet formation by flow instabilities between immiscible fluids: (a) T-junction droplet generator and (b) photomicrograph of water-in-oil emulsion formation (Reprinted from [146] with permission. Copyright 2001 by the American Physical Society). (c) Flow focusing configuration, and (d) formation of the water-in-oil droplets (Reproduced from [147] by permission of The Royal Society of Chemistry)

[150]. The two phases are forced through a narrow region (orifice) located downstream of the three channels. The effects of pressure and shear stress exerted on the inner fluid cause the formation of a thin neck that eventually collapses, leading to the formation of a droplet. In this design, the flow rates of the two phases and their viscosity play crucial roles in controlling droplet generation [150].

Generally speaking, mixing inside microdroplets is enhanced by a reduction in diffusion length and by the intimate contact between the fluids to be mixed due to the geometrical confinement of the droplet itself. Furthermore, the contact between the droplet surface and the channel walls causes the generation of recirculating flow within the droplet fluid [137] (Fig. 15). When the droplet is transported through a straight channel, these flows are generated in the two halves of the channel. Each flow pattern consists of two counter-circulating flows. This flow pattern provides a mixing of the two halves; however, mass transport is not

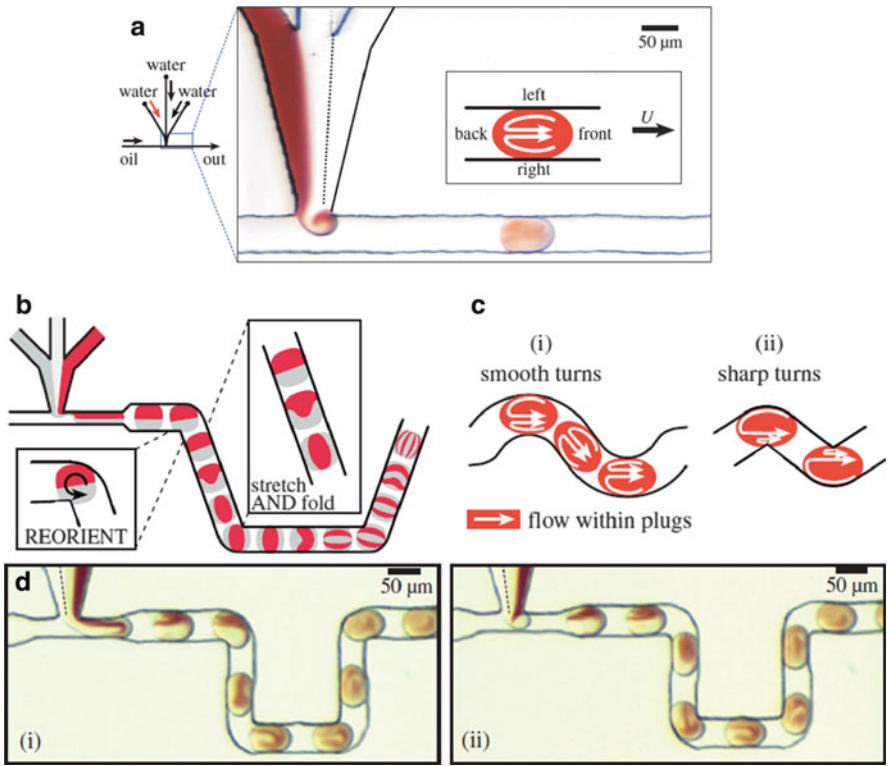


**Fig. 15** Mixing in microdroplets flowing in a microchannel: (a) Recirculation flow generated in a straight channel. (b, c) Mixing patterns generated in winding channels that causes (b) stretch, fold, and reorientation of the fluids interface and (c) asymmetrical recirculation patterns in the droplet halves. (d) Experimental results showing the chaotic advection thus generated in microdroplets (Adapted from [151] with permission)



activated between the two halves that thus remain separated and unmixed [137] (Fig. 15a). In order to create chaotic advection within the whole volume of the microdroplets, the channel geometry must be varied in order to stretch and fold the liquid in the droplets [53].

A classic passive way to introduce chaotic advection relies on the introduction of turns and bends in the channel in order to introduce unequal recirculating flow in each half of the droplet. This type of micromixer is known as a planar serpentine micromixer (PSM). When a droplet is driven through a winding channel, each half is in contact with a different section of the turn. The half that is exposed to the inner arc is in contact with a shorter section, while the other is in contact with the larger section of the outer arc. Within the half exposed to the inner part, a smaller recirculating flow is generated compared with the other half. This asymmetrical distribution of the recirculating flows in combination with the alternate switching of them therefore causes chaos and crossing of fluid streams (Fig. 15c) [53, 139, 151, 152]. Furthermore, the turn in the winding channel causes the interface between the two halves of the plug to be reoriented from the direction of plug movement, leading to an exponentially thinner striation between the two fluids to be mixed (Fig. 15b). It must be noted that the extent of mixing can be controlled by controlling the number of turn in the microchannel.

Interestingly, has been reported that a combination of very high relative viscosity of disperse and continuous phases, together with the use of surface active molecules, caused a combination of slug flow and fine droplet dispersion, providing efficient mixing and increasing the interfacial area between the two phases [153]. This mechanism was particularly useful in enhancing the reaction rate of interfacial reactions, such as lipase-catalyzed acetyl isoamyl acetate synthesis [153].

Other channel geometries to induce chaotic advection in microdroplets have also been developed. Liao et al. [154] proposed the introduction of bumps on one side of the channel wall to promote droplet deformation. The authors proposed that the enhancement of mixing could be addressed to the thinning of the lubricant layer of dispersant fluid and by the interfacial stress induced by the bumps. A similar approach was presented by Liao et al. [154]. However, in this case the bumps were introduced in both the lateral channels walls. Similarly, Tung et al. [155] proposed the introduction of a nonuniform cross-section of the wall to deform the microdroplets and enhance the mixing.

### 3.2 Active Micromixers

As described previously, active micromixers rely on an external energy input to introduce perturbation within the fluid streamlines to achieve mixing. Therefore, they are categorized with respect to the type of external perturbation energy:

1. Pressure field
2. Electrokinetic

3. Dielectrophoretic
4. Electrowetting
5. Magneto-hydrodynamic
6. Ultrasound

### 3.2.1 Pressure Field Disturbance

One of the simple ways to achieve active mixing is to induce a pressure field disturbance. Active micromixers relying on this strategy have been reported from different authors [43, 156–159]. Deshmuck et al. [156, 157] proposed a T-junction microfluidic chip with an integrated micropump that alternatively drives and stops the flow within the microdevice to create a segmented flow.

A similar approach was presented by Glasgow et al. [43] (Fig. 16) that proposed the use of a pulsing velocity fluid altering periodically the flow rate in the inlet channel from high to low. The author used a simple T-shaped mixer to demonstrate the effectiveness of this method at very low  $Re$  (from 0.30 to 2.55). They also demonstrated that when both inlets were pulsed simultaneously the interface between the two liquid was stretched through the confluence zone, leading to an enhanced mixing. The authors also showed the influence of the amount and periodicity of the pulsing on mixing efficiency, reporting that the best results were obtained when the pulsing had a phase difference of  $180^\circ$ . Lei et al. [160] reported a microfluidic mixer based on the same concept of fluid discretization and operated by two vortex micropumps. The discretized fluid, constituted of discrete volumes of liquids to be mixed, is then pumped into an expansion chamber to increase the interfacial surface area between the volumes. The flow in the micro-mixer had an  $Re$  of 30.

### 3.2.2 Electrokinetic Disturbance

Electrokinetic instability (EKI) (or disturbance) micromixers take advantage of fluctuating electric field to induce mixing in microfluidic channels or chambers [161–163]. The fluctuating electric fields cause rapid stretching and folding of the fluids interfaces that are able to stir the fluid stream in highly laminar flow ( $Re < 1$ ) [161]. Different mixing strategies that implement EKI have been presented. Oddy et al. [161] reported a pressure-driven micromixer (i.e., connected with syringe pump) in which oscillating electroosmotic flows were induced by an alternating current voltage (Fig. 17). A periodically alternated flow approach was also presented for an electroosmotic-driven flow device by using either a nonuniform zeta potential along the walls [164] or by varying the voltage with time [165, 166].

Recently, it has also been reported that EKI mixing effectiveness can be enhanced by combining its action with a passive micromixing strategy using channel geometries

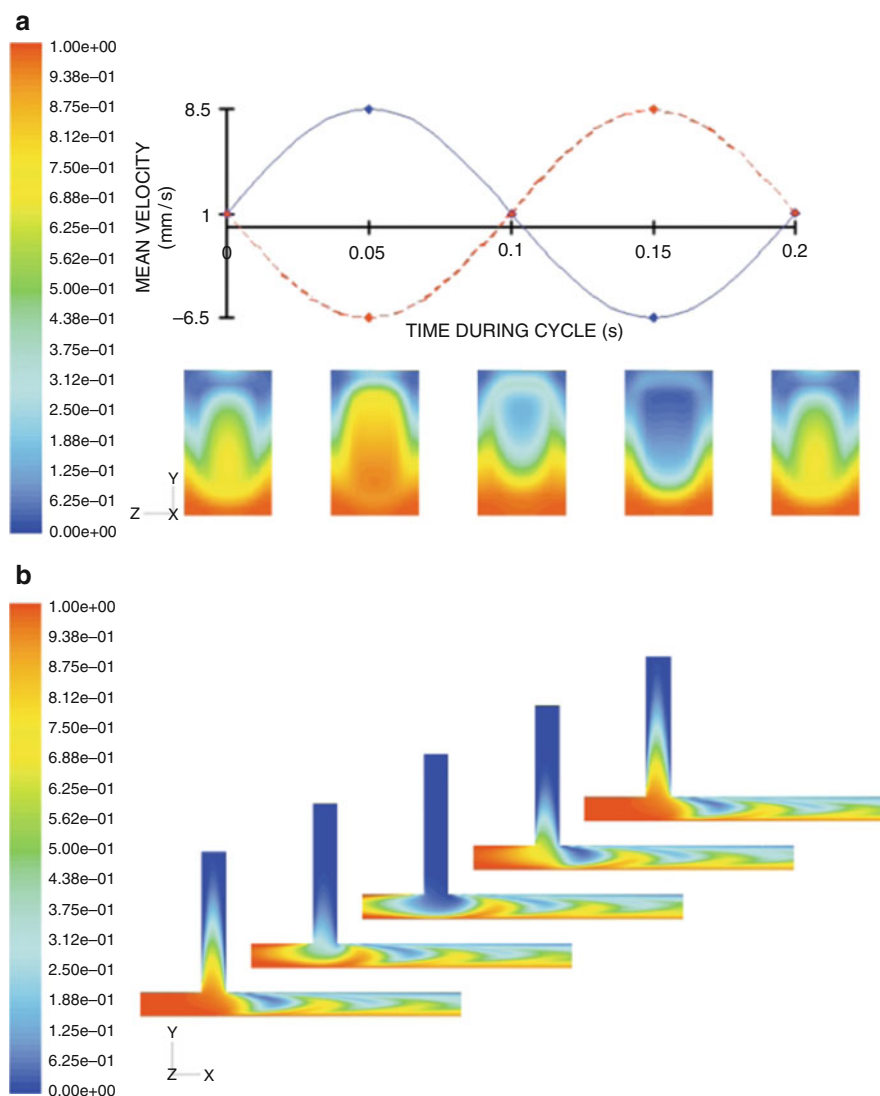


**Fig. 16** Mixing by pressure field disturbance: (a) Mean fluid velocity along the channel as function of time for in-line inlet and perpendicular inlet. The fluids are pulsed with a simulated  $180^\circ$  phase difference. Contour levels of mass fraction of the fluids in the Y-Z plane are shown. (b) Contour levels in the Y-X plane as a function of time as expressed in the graph in (a). Alternate puffs of fluids are created as result of the pulsation introduced within the fluid stream (Reproduced from [43] by permission of The Royal Society of Chemistry)

that induce secondary flow [167]. Results show that for a 10-mm long T-type mixer combining active and passive mixing strategies, the mixing efficiency can be enhanced from 50% to 90% with respect to the solely active mixing strategy.

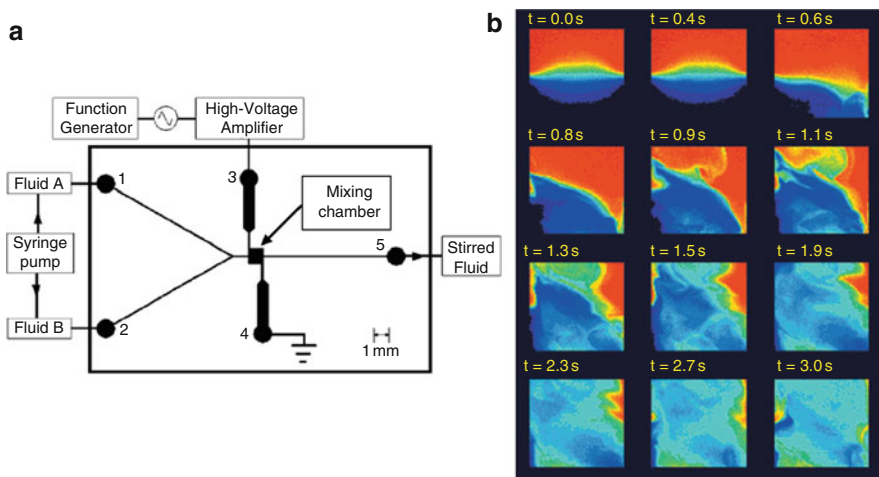


**Fig. 17** Electrokinetic instability micromixer. (a) EKI micromixer. Fluids are pumped from inlets 1 and 2, and flow toward outlet 5, passing through the square mixing chamber. Side ports 3 and 4 allow for AC excitation. The mixing effect is confined within the mixing chamber. (b) Complex fluid motion generated within the mixing chamber after the application of the AC field causes rapid stretching and folding of the fluid interface, thus enhancing the mixing (Adapted from [161] with permission. Copyright 2001 American Chemical Society)

### 3.2.3 Dielectrophoretic Disturbance

Dielectrophoresis is a phenomenon in which polarization of particle is induced by a nonuniform electric field. Polarized particles can move towards or away from the electrodes in response to the electrical field applied. A synergistic effect between the movement of the particles and the geometry of the channel causes the creation of chaotic advection that causes the mixing of the fluid surrounding the particle. This approach was explored by different research groups in the last decade [168–170].

Recently, a similar approach based on isotachophoresis was reported in a microfluidic device, demonstrating its usefulness for micromixing purposes [170]. The author demonstrated that a small sample volume could be brought in contact in a controllable manner to trigger a fairly fast mixing. This type of mixer does not require complicated geometry and could be particular useful in the field of digital microfluidics.

### 3.2.4 Electrowetting Shaking

As described in the passive mixer section, movement of liquid droplets can generate flow patterns within the fluid and enhance the mixing of species inside the droplets. An active way to induce mixing in droplets is represented by electrowetting on dielectrics (EWOD), or simply electrowetting. EWOD relies on the control of the interfacial tension of a droplet by means of an electric field. Droplets containing different species can be electrically actuated to coalesce using electrowetting effect. After the coalescence, diffusion begins in the droplet and mixing of the two fluid

species occurs. However, this passive-like mixing is rather slow [171]. To speed up the mixing process, different authors [171–173] have proposed the use of electro-wetting to shake, split, and merge the droplets in order to create recirculating patterns that increase the interfacial area between the two liquids to be mixed. The droplets act as virtual mixing chambers, and mixing occurs by oscillating the droplet across a number of electrodes at various frequencies. The authors demonstrated an increase in mixing as the number of electrodes and transport velocity of the droplet increase [171]. Furthermore, it must be noted that EWOD can achieve mixing in a much more confined space than channel-based mixing.

### 3.2.5 Magneto-Hydrodynamic Disturbance

Magneto-hydrodynamic (MHD) disturbance relies on the induction of Lorentz body forces in an electrolyte solution [46, 174, 175]. MHD devices utilize an array of electrodes deposited in the channel walls to create current flows within the fluid to be mixed, in the presence of an alternate potential difference on the electrode pair. By coupling the generated electric field with a magnetic field, Lorentz body force could be generated. The complex flow field generated deforms and stretches the material interface, enhancing the mixing (Fig. 18).

### 3.2.6 Ultrasound Disturbance

Mixing can be achieved by means of acoustic stirring created by ultrasonic waves [42, 44, 176–181]. Ultrasounds are introduced into the channel by integrated piezoelectric ceramic transducers [42, 44, 176, 177]. The ultrasonic action causes an acoustic stirring of the fluid perpendicular to the flow direction and leads to an enhancement of the mixing inside the microfluidic channel [42] or chamber [44, 180]. A turbulent-like mixing was achieved at  $Re < 1$ .

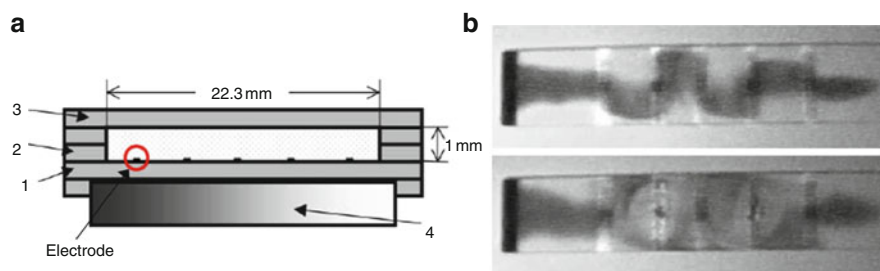


**Fig. 18** Magneto-hydrodynamic disturbance (MHD) micromixer. (a) Cross-section view of an MHD mixer. MHD mixer comprises the following layers: (1) channel bottom wall containing the electrodes; (2) spacer layers that constitute the mixing chamber; (3) cover plates; (4) permanent magnet. (b) Deformation of fluid stream resulting from the application of a Lorentz body force (*upper panel*) and corresponding creation of eddies (*lower panel*) (Reprinted from [46] with permission. Copyright 2001 Elsevier)

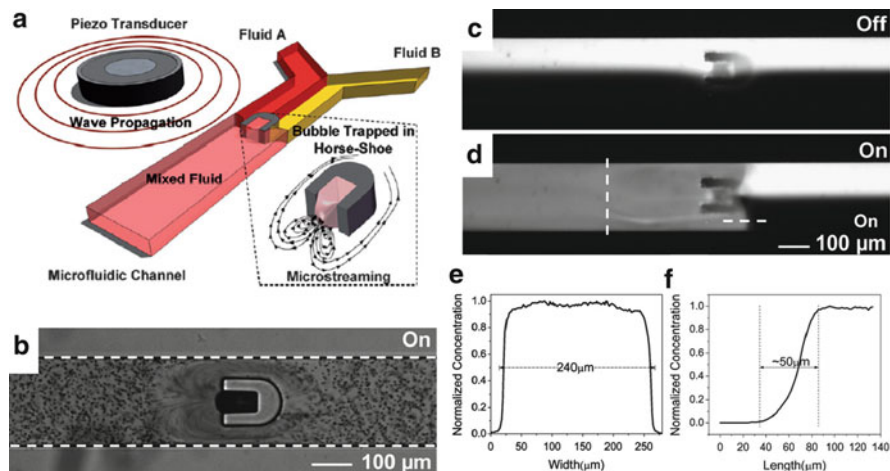


**Fig. 19** Mixing by acoustic microstreaming. (a) Micromixer. An air bubble is trapped within the horseshoe structure and when activated by the piezo transducer generates a microstreaming around it, as shown in the *inset*. (b) Photomicrograph showing microstreaming. (c) No mixing effect was observed in the absence of acoustic waves. (d) Fast mixing was achieved in the presence of acoustic waves. Concentration plots (e) across the channel width and (f) near the bubble (Reproduced from [181] by permission of The Royal Society of Chemistry)

Air bubbles can be introduced in a microfluidic mixer in order to enhance the mixing process. The surface of an air bubble in a liquid medium exposed to a sound field can act as a vibrating membrane. The membrane vibration causes a bulk fluid movement at the air–liquid interface. This effect, known as cavitation microstreaming, has been applied in microfluidic micromixers using a single bubble [181] (Fig. 19) or an array of bubbles [178, 179].

### 3.2.7 Other Types of Active Micromixers

Thermal disturbance micromixers rely either on the increase in the diffusion coefficient due to a temperature increase, or on natural convection to enhance the mixing in the microfluidic channel [45, 182]. Recently Kim et al. [182] reported a pumpless micromixer based on thermal disturbance and applied it to perform a polymerase chain reaction (PCR).

Stirring in microdevices can also be achieved by means of micro-sized moving elements that create a turbulent flow within the fluid to be mixed [183–185]. These devices allow rapid mixing of a large volume of sample within the characteristic length of the microstirring elements and can be used with a wide range of fluids. Lu et al. [183] reported the use of a rotating bar made of ferromagnetic material driven by means of an external rotating magnetic field. A similar approach was developed by Huh et al. [185] and applied for sensing infectious viral disease. The system proposed used a rotating micromagnetic disk driven by a commercial rotating magnet.

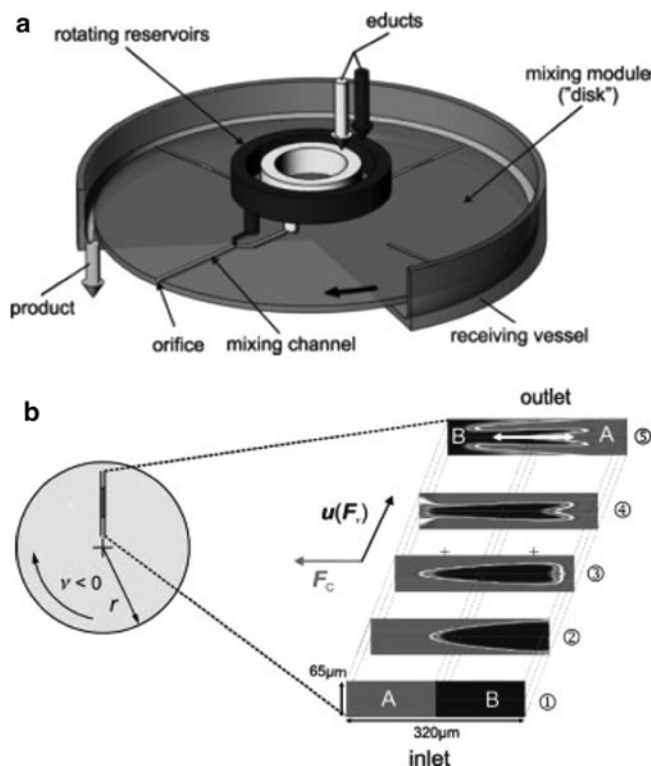


**Fig. 20** Centrifugal micromixer. (a) Micromixer device and its components. (b) Simulation of the mixing process shows the effect of the Coriolis pseudoforce ( $F_c$ ) in folding the interface of the two liquids. Simultaneously, the centrifugal force ( $F_v$ ) drives the liquid toward the outlet (Reproduced from [186] with permission. Copyright Wiley-VCH)

Another novel micromixer was presented by Haeberle et al. [186]. It consisted of a modular centrifugal micromixer (Fig. 20) relying on the force generated by the rotating drive to provide both pumping and mixing energies. The mixing is due to the Coriolis force, which causes the interface between the two liquids to be mixed to folds and therefore increases the contact surface between them. The micromixer consists of a planar rotating disk hosting the mixing channel, a rotating unit (standard laboratory centrifuge), and a contact-free reservoir. This mixing system has a high volume throughput on the order of milliliters per minute.

## 4 Why Microfluidic Mixers?

The intense research over the last two decades on developing microfluidic-based mixers was driven by the possibility to leverage a number of advantages that stem from the unique fluid behavior in a microfluidic environment. At microscale level,

fluid properties become increasingly controlled and provide the possibility of exerting control over the different processes carried out in a microfluidic environment.

First, the degree of mixing of reactants could greatly influence the product composition for very fast reactions, as demonstrated for both macro- [187, 188] and microreactors [74, 77]. In this respect, micromixers are appealing tools since they can provide a fast and controllable mixing process as a result of their small dimension and the omnipresence of a highly predictable laminar flow. These properties make micromixers particularly applicable for reactions with very fast kinetics or for dealing with unstable intermediate substances [56, 189]. The fast mixing process is also a valuable advantage for precipitation/crystallization processes such as production of colloidal systems or nanoparticles [190]. Fast mixing provided by micromixers can also be exploited to obtain a freeze-quenching process that allows trapping of metastable intermediates during fast chemical or biochemical reactions [117].

Microfluidic systems also provide the possibility to spatially and temporally monitor and control reactions by adding reagents at precise time intervals during the reaction progress. This was demonstrated by Shestopalov et al. [191] by carrying out a multistep synthesis of quantum dots using the microfluidic droplet reactor.

The small internal volume also provides an opportunity to decrease the amount of sample required for the analysis or reaction. This is particularly useful when rare and valuable substances or samples are used, as well as when a large number of samples in a limited small volume are available for biological and chemical analysis and screening [56].

Typically, microfluidic devices have channels with dimensions between 10 and 400  $\mu\text{m}$ . This small dimension compared to conventional mixing systems results in an increase in the surface-to-volume ratio, to 10,000–50,000  $\text{m}^2 \text{m}^{-3}$  compared with 100–2,000  $\text{m}^2 \text{m}^{-3}$  of their macroscale counterparts. This characteristic endows micromixers with a superior heat transfer and control [192], allowing reactions to be performed in an isothermal manner [83, 193, 194]. Due to their heat transfer efficiency, micromixers can be conveniently applied for handling reactions in which fast heating and cooling of the reaction mixture are required, such as highly exothermal reactions [9, 195–199].

Recently, the development of microfluidic systems that are able to controllably generate liquid droplets has defined the possibility to perform a diverse range of chemical and biological processes, including the synthesis of biomolecules, drug delivery systems, and diagnostic testing [149, 200]. Microfluidic devices are able to generate highly monodisperse droplets [201–203] in a parallelized fashion, in line with industrial applications, and avoid cross contamination between the droplets by separating the droplets with an immiscible fluid or gas [201, 203]. Digital or droplet microfluidics is particular interesting because it allows the handling of each droplet as a singular microreactor that can be individually controlled and analyzed in an high-throughput fashion [204, 205]. The confinement of the substances in discrete droplets also allows the elimination of residence time variation due to the parabolic flow profile that frustrates single-phase microfluidic mixers [206].

In general, the small internal volume of the micromixers is beneficial in a safety-related point of view when handling hazardous substances and chemical reactions



[198]. The possibility of generation on-demand and in-situ of hazardous and toxic substances (e.g.,  $H_2O_2$ ) represents an important advantage [207].

Lastly, it must be noted that another important driving force in developing microfluidic based mixers and reactors is represented by their possible application as elements of more complicated and multifunctional  $\mu$ TAS.

## 5 Conclusions

Research on microfluidics and  $\mu$ TAS has been progressing rapidly in the last two decades. Micromixers represent one of the essential components in integrated microfluidic systems for chemical, biological, and medical applications. This chapter describes the characteristics of the microfluidic environment and the peculiar fluid behavior at the microscale. Among the different features of fluid at the microscale, one of the most relevant to mixing applications is the omnipresence of laminar flow where mixing can be dominantly accomplished by molecular diffusion. Nevertheless, this apparent disadvantage coupled with the reduced dimension of microfluidic devices has been leveraged to provide faster and controllable mixing. Design and characterization of various microfluidic mixers have been reported, and their operation conditions and implications for mixing at microscale have been discussed.

The mixing principles applied can be categorized into two groups, active and passive. Passive micromixers rely solely on pumping energy to manipulate the fluid interface and enhance mixing. Passive micromixers are then divided into different categories that reflect the way in which fluid streams are manipulated in order to increase mixing. Specifically, T- or Y-shaped micromixers, parallel lamination micromixers, focusing enhanced mixers, sequential lamination micromixers, chaotic advection micromixers, and droplet micromixers have been discussed.

Active micromixers use an external energy source to introduce perturbation in the fluid stream and are then categorized with respect to the type of energy source used. Pressure field, electrokinetic, dielectrophoretic, electrowetting shaking, magneto-hydrodynamic, ultrasound, and thermal-assisted micromixers have been presented and discussed.

Finally, the practical advantages of mixing on the microscale have been discussed, showing that microfluidic technology provides a useful approach for solving a number of practical issues for chemical, biological and medical applications. Nevertheless, micromixing technology is still mostly focused on laboratory applications because the possible industrial applications are still frustrated by a lack of understanding of scalability, profitability, and operational flexibility.

Owing to the excellent capability of microfluidic devices and the presence of micromixer technology that has been studied in depth, it can be anticipated that in the near future more practical laboratory and industrial applications for micromixers will be developed.

## References

1. Ståhl M, Åslund B, Rasmuson Å (2001) Reaction crystallization kinetics of benzoic acid. *AIChE J* 47(7):1544–1560
2. Schwarzer H, Schwertfirt F, Manhart M, Schmid H, Peukert W (2006) Predictive simulation of nanoparticle precipitation based on the population balance equation. *Chem Eng Sci* 61(1): 167–181
3. Mae K, Maki T, Hasegawa I, Eto U, Mizutani Y, Honda N (2004) Development of a new micromixer based on split/recombination for mass production and its application to soap free emulsifier. *Chem Eng J* 101(1–3):31–38
4. Okubo Y, Toma M, Ueda H, Maki T, Mae K (2004) Microchannel devices for the coalescence of dispersed droplets produced for use in rapid extraction processes. *Chem Eng J* 101 (1–3):39–48
5. Sprogies T, Köhler J, Gross G (2008) Evaluation of static micromixers for flow-through extraction by emulsification. *Chem Eng J* 135:S199–S202
6. Iwasaki T, Yoshida J (2005) Free radical polymerization in microreactors. Significant improvement in molecular weight distribution control. *Macromolecules* 38(4):1159–1163
7. Nagaki A, Kawamura K, Suga S, Ando T, Sawamoto M, Yoshida J (2004) Cation pool-initiated controlled/living polymerization using microsystems. *J Am Chem Soc* 126(45): 14702–14703
8. Nagaki A, Tomida Y, Yoshida J (2008) Microflow-system-controlled anionic polymerization of styrenes. *Macromolecules* 41(17):6322–6330
9. Wilms D, Klos J, Frey H (2008) Microstructured reactors for polymer synthesis: a renaissance of continuous flow processes for tailor-made macromolecules? *Macromol Chem Phys* 209(4):343–356
10. Haswell S, Middleton R, O'Sullivan B, Skelton V, Watts P, Styring P (2001) The application of micro reactors to synthetic chemistry. *Chem Commun* (5):391–398
11. Hessel V, Hofmann C, Löb P, Löndorf J, Löwe H, Ziegler A (2005) Aqueous Kolbe-Schmitt synthesis using resorcinol in a microreactor laboratory rig under high-p, T conditions. *Org Process Res Dev* 9(4):479–489
12. Kee S, Gavriiliadis A (2007) Batch versus continuous mg-scale synthesis of chalcone epoxide with soluble polyethylene glycol poly-L-leucine catalyst. *J Mol Catal A Chem* 263(1–2):156–162
13. Miller E, Wheeler A (2008) A digital microfluidic approach to homogeneous enzyme assays. *Anal Chem* 80(5):1614–1619
14. Ukita Y, Asano T, Fujiwara K, Matsui K, Takeo M, Negoro S, Kanie T, Katayama M, Utsumi Y (2008) Application of vertical microreactor stack with polystyrene microbeads to immunoassay. *Sens Actuators A Phys* 145:449–455
15. Bilsel O, Kayatekin C, Wallace L, Matthews C (2005) A microchannel solution mixer for studying microsecond protein folding reactions. *Rev Sci Instrum* 76:014302
16. Park T, Lee S, Seong G, Choo J, Lee E, Kim Y, Ji W, Hwang S, Gweon D (2005) Highly sensitive signal detection of duplex dye-labelled DNA oligonucleotides in a PDMS microfluidic chip: confocal surface-enhanced Raman spectroscopic study. *Lab Chip* 5(4):437–442
17. Maerkl S (2009) Integration column: microfluidic high-throughput screening. *Integr Biol* 1(1):19–29
18. Chen X, Cui D, Liu C, Li H, Chen J (2007) Continuous flow microfluidic device for cell separation, cell lysis and DNA purification. *Anal Chim Acta* 584(2):237–243
19. Zhang C, Xing D, Li Y (2007) Micropumps, microvalves, and micromixers within PCR microfluidic chips: advances and trends. *Biotechnol Adv* 25(5):483–514
20. Sato K, Hibara A, Tokeshi M, Hisamoto H, Kitamori T (2003) Microchip-based chemical and biochemical analysis systems. *Adv Drug Deliv Rev* 55(3):379–391
21. Malic L, Herrmann M, Hoa X, Tabrizian M (2007) Current state of intellectual property in microfluidic nucleic acid analysis. *Recent Pat Eng* 1(1):71–88

22. Ingham C, Vlieg J (2008) MEMS and the microbe. *Lab Chip* 8(10):1604–1616
23. Micheletti M, Lye G (2006) Microscale bioprocess optimisation. *Curr Opin Biotechnol* 17(6):611–618
24. Schäpper D, Alam M, Szita N, Eliasson Lantz A, Gernaey K (2009) Application of microbioreactors in fermentation process development: a review. *Anal Bioanal Chem* 395(3):679–695
25. Schulte T, Bardell R, Weigl B (2002) Microfluidic technologies in clinical diagnostics. *Clin Chim Acta* 321(1–2):1–10
26. Rapp B, Gruhl F, Länge K. (2010) Biosensors with label-free detection designed for diagnostic applications. *Anal Bioanal Chem* 398:2403–2412
27. Zafar Razzacki S, Thwar P, Yang M, Ugaz V, Burns M (2004) Integrated microsystems for controlled drug delivery. *Adv Drug Deliv Rev* 56(2):185–198
28. Reyes D, Iossifidis D, Auroux P, Manz A (2002) Micro total analysis systems. 1. Introduction, theory, and technology. *Anal Chem* 74(12):2623–2636
29. Lee S, Lee S (2004) Micro total analysis system ( $\mu$ -TAS) in biotechnology. *Appl Microbiol Biotechnol* 64(3):289–299
30. Dittrich P, Tachikawa K, Manz A (2006) Micro total analysis systems. Latest advancements and trends. *Anal Chem* 78(12):3887–3908
31. Zhang Y, Ozdemir P (2009) Microfluidic DNA amplification – a review. *Anal Chim Acta* 638(2):115–125
32. Doku G, Verboom W, Reinhoudt D, van den Berg A (2005) On-microchip multiphase chemistry – a review of microreactor design principles and reagent contacting modes. *Tetrahedron* 61(11):2733–2742
33. Naher S, Orpen D, Brabazon D, Morshed M (2010) An overview of microfluidic mixing application. *Adv Mat Res* 83:931–939
34. Dittrich P, Manz A (2006) Lab-on-a-chip: microfluidics in drug discovery. *Nat Rev Drug Discov* 5(3):210–218
35. Yoshida J, Nagaki A, Iwasaki T, Suga S (2005) Enhancement of chemical selectivity by microreactors. *Chem Eng Technol* 28(3):259–266
36. Baldyga J, Pohorecki R (1995) Turbulent micromixing in chemical reactors – a review. *Chem Eng J Biochem Eng J* 58(2):183–195
37. Beebe DJ, Mensing GA, Walker GM (2002) Physics and application of microfluidic in biology. *Annu Rev Biomed Eng* 4:261–286
38. Weigl B, Bardell R, Cabrera C (2003) Lab-on-a-chip for drug development. *Adv Drug Deliv Rev* 55(3):349–377
39. Nguyen N, Wereley S (2002) Fundamentals and applications of microfluidics. Artech House, Norwood
40. Einstein A, Fürth R (1956) Investigations on the theory of the Brownian movement. Dover Publications, New York
41. Zhang Z, Zhao P, Xiao G, Lin M, Cao X (2008) Focusing-enhanced mixing in microfluidic channels. *Biomicrofluidics* 2:014101
42. Yaralioglu G, Wygant I, Marentis T, Khuri-Yakub B (2004) Ultrasonic mixing in microfluidic channels using integrated transducers. *Anal Chem* 76(13):3694–3698
43. Glasgow I, Aubry N (2003) Enhancement of microfluidic mixing using time pulsing. *Lab Chip* 3(2):114–120. <http://dx.doi.org/10.1039/B302569A>
44. Yang Z, Matsumoto S, Goto H, Matsumoto M, Maeda R (2001) Ultrasonic micromixer for microfluidic systems. *Sens Actuators A Phys* 93(3):266–272
45. Tsai H Jr, Lin L (2002) Active microfluidic mixer and gas bubble filter driven by thermal bubble micropump\* 1. *Sens Actuators A Phys* 97:665–671
46. Bau H, Zhong J, Yi M (2001) A minute magneto hydro dynamic (MHD) mixer. *Sens Actuators B Chem* 79(2–3):207–215
47. Wu Z, Nguyen N (2005) Convective–diffusive transport in parallel lamination micromixers. *Microfluid Nanofluid* 1(3):208–217
48. Nguyen N, Wu Z (2005) Micromixers – a review. *J Micromech Microeng* 15:R1

49. Kamholz A, Yager P (2002) Molecular diffusive scaling laws in pressure-driven microfluidic channels: deviation from one-dimensional Einstein approximations. *Sens Actuators B Chem* 82(1):117–121
50. Schwesinger N, Frank T, Wurmus H (1996) A modular microfluid system with an integrated micromixer. *J Micromech Microeng* 6:99
51. Knight J, Vishwanath A, Brody J, Austin R (1998) Hydrodynamic focusing on a silicon chip: mixing nanoliters in microseconds. *Phys Rev Lett* 80(17):3863–3866
52. Günther A, Jhunjhunwala M, Thalmann M, Schmidt M, Jensen K (2005) Micromixing of miscible liquids in segmented gas-liquid flow. *Langmuir* 21(4):1547–1555
53. Song H, Tice J, Ismagilov R (2003) A microfluidic system for controlling reaction networks in time. *Angew Chem* 115(7):792–796
54. Johnson T, Ross D, Locascio L (2002) Rapid microfluidic mixing. *Anal Chem* 74(1):45–51
55. Stroock A, Dertinger S, Ajdari A, Mezic I, Stone H, Whitesides G (2002) Chaotic mixer for microchannels. *Science* 295(5555):647
56. Hessel V, Löwe H, Schönfeld F (2005) Micromixers – a review on passive and active mixing principles. *Chem Eng Sci* 60(8–9):2479–2501
57. Jeong G, Chung S, Kim C, Lee S (2010) Applications of micromixing technology. *Analyst* 135(3):460–473
58. Kamholz A, Weigl B, Finlayson B, Yager P (1999) Quantitative analysis of molecular interaction in a microfluidic channel: the T-sensor. *Anal Chem* 71(23):5340–5347
59. Gobby D, Angeli P, Gavriilidis A (2001) Mixing characteristics of T-type microfluidic mixers. *J Micromech Microeng* 11:126
60. Ismagilov R, Stroock A, Kenis P, Whitesides G, Stone H (2000) Experimental and theoretical scaling laws for transverse diffusive broadening in two-phase laminar flows in microchannels. *Appl Phys Lett* 76:2376
61. Soleymani A, Kolehmainen E, Turunen I (2008) Numerical and experimental investigations of liquid mixing in T-type micromixers. *Chem Eng J* 135:S219–S228
62. Wong S, Bryant P, Ward M, Wharton C (2003) Investigation of mixing in a cross-shaped micromixer with static mixing elements for reaction kinetics studies. *Sens Actuators B Chem* 95(1–3):414–424
63. Wong S, Ward M, Wharton C (2004) Micro T-mixer as a rapid mixing micromixer. *Sens Actuators B Chem* 100(3):359–379
64. Hoffmann M, Raebiger N, Schlueter M, Blazy S, Bothe D, Stemich C, Warnecke A (2003) Experimental and numerical investigations of T-shaped micromixers. In: *Proceedings of the 11th European conference on mixing, Bamberg, Germany, 14–17 October 2003*, pp 269–276
65. Veenstra T, Lammerink T, Elwenspoek M, Berg A (1999) Characterization method for a new diffusion mixer applicable in micro flow injection analysis systems. *J Micromech Microeng* 9:199
66. Erbacher C, Bessoth F, Busch M, Verpoorte E, Manz A (1999) Towards integrated continuous-flow chemical reactors. *Microchim Acta* 131(1):19–24
67. Lob P, Drese K, Hessel V, Hardt S, Hofmann C, Lowe H, Schenk R, Schönfeld F, Werner B (2004) Steering of liquid mixing speed in interdigital micro mixers-from very fast to deliberately slow mixing. *Chem Eng Technol* 27(3):340–345
68. Cha J, Kim J, Ryu S, Park J, Jeong Y, Park S, Kim H, Chun K (2006) A highly efficient 3D micromixer using soft PDMS bonding. *J Micromech Microeng* 16:1778. <http://dx.doi.org/10.1088/0960-1317/16/9/004>
69. Che-Hsin L, Chien-Hsiung T, Lung-Ming F (2005) A rapid three-dimensional vortex micromixer utilizing self-rotation effect under low Reynolds number conditions. *J Micromech Microeng* 15:935. <http://dx.doi.org/10.1088/0960-1317/15/5/006>
70. Bessoth F, deMello A, Manz A (1999) Microstructure for efficient continuous flow mixing. *Anal Commun* 36(6):213–215
71. Floyd T, Schmidt M, Jensen K (2005) Silicon micromixers with infrared detection for studies of liquid-phase reactions. *Ind Eng Chem Res* 44(8):2351–2358

72. Jackman R, Floyd T, Ghodssi R, Schmidt M, Jensen K (2001) Microfluidic systems with on-line UV detection fabricated in photodefinable epoxy. *J Micromech Microeng* 11:263
73. Drese K (2004) Optimization of interdigital micromixers via analytical modeling – exemplified with the SuperFocus mixer. *Chem Eng J* 101(1–3):403–407
74. Ehlers S, Elgeti K, Menzel T, Wießmeier G (2000) Mixing in the offstream of a micro-channel system\* I. *Chem Eng Process* 39(4):291–298
75. Hardt S, Schönfeld F (2003) Laminar mixing in different interdigital micromixers: II. Numerical simulations. *AIChE J* 49(3):578–584
76. Hessel V, Hardt S, Löwe H, Schönfeld F (2003) Laminar mixing in different interdigital micromixers: I. Experimental characterization. *AIChE J* 49(3):566–577
77. Ehrfeld W, Golbig K, Hessel V, Lowe H, Richter T (1999) Characterization of mixing in micromixers by a test reaction: single mixing units and mixer arrays. *Ind Eng Chem Res* 38(3):1075–1082
78. Rosenfeld C, Serra C, Brochon C, Hadziioannou G (2007) High-temperature nitroxide-mediated radical polymerization in a continuous microtube reactor: towards a better control of the polymerization reaction. *Chem Eng Sci* 62(18–20):5245–5250
79. Rosenfeld C, Serra C, Brochon C, Hessel V, Hadziioannou G (2008) Use of micromixers to control the molecular weight distribution in continuous two-stage nitroxide-mediated copolymerizations. *Chem Eng J* 135:S242–S246
80. Chung Y, Hsu Y, Jen C, Lu M, Lin Y (2004) Design of passive mixers utilizing microfluidic self-circulation in the mixing chamber. *Lab Chip* 4(1):70–77
81. Lin C, Tsai C, Fu L (2005) A rapid three-dimensional vortex micromixer utilizing self-rotation effects under low Reynolds number conditions. *J Micromech Microeng* 15:935
82. Ehrfeld W, Hessel V, Haverkamp V (2000) Microreactors. In: Ullmann's encyclopedia of industrial chemistry. Wiley-VCH, Weinheim. doi: 10.1002/14356007.b16\_b37
83. Jähnisch K, Hessel V, Löwe H, Baerns M (2004) Chemistry in microstructured reactors. *Angew Chem Int Ed* 43(4):406–446
84. Lee S, Kim D, Lee S, Kwon T (2006) A split and recombination micromixer fabricated in a PDMS three-dimensional structure. *J Micromech Microeng* 16:1067. <http://dx.doi.org/10.1088/0960-1317/16/5/027>
85. Fang W, Yang J (2009) A novel microreactor with 3D rotating flow to boost fluid reaction and mixing of viscous fluids. *Sens Actuators B Chem* 140(2):629–642
86. Branebjerg J, Gravesen P, Krog J, Nielsen C (2002) Fast mixing by lamination. In: Proceedings IEEE 9th annual international workshop on micro electro mechanical systems (MEMS'96), San Diego, CA, 11–15 February 2002, pp 441–446
87. Hardt S, Pennemann H, Schönfeld F (2006) Theoretical and experimental characterization of a low-Reynolds number split-and-recombine mixer. *Microfluid Nanofluid* 2(3):237–248
88. Munson M, Yager P (2004) Simple quantitative optical method for monitoring the extent of mixing applied to a novel microfluidic mixer. *Anal Chim Acta* 507(1):63–71
89. Radadia A, Cao L, Jeong H, Shannon M, Masel R (2008) A 3D micromixer fabricated with dry film resist. In: Proceedings IEEE 20th international conference on micro mechanical systems (MEMS'07), Hyogo, Japan, 21–25 January 2007, pp 361–364
90. Schönfeld F, Hessel V, Hofmann C (2004) An optimised split-and-recombine micro-mixer with uniform 'chaotic' mixing. *Lab Chip* 4(1):65–69
91. Bertsch A, Heimgartner S, Cousseau P, Renaud P (2001) Static micromixers based on large-scale industrial mixer geometry. *Lab Chip* 1(1):56–60. <http://dx.doi.org/10.1039/DOI/B103848F>
92. Lim T, Son Y, Jeong Y, Yang D, Kong H, Lee K, Kim D (2010) Three-dimensionally crossing manifold micro-mixer for fast mixing in a short channel length. *Lab Chip* 11(1):100–103. <http://dx.doi.org/10.1039/DOI/C005325M>
93. Melin J, Giménez G, Roxhed N, Wijngaart W, Stemme G (2004) A fast passive and planar liquid sample micromixer. *Lab Chip* 4(3):214–219
94. He B, Burke B, Zhang X, Zhang R, Regnier F (2001) A picoliter-volume mixer for microfluidic analytical systems. *Anal Chem* 73(9):1942–1947

95. Sudarsan A, Ugaz V (2006) Multivortex micromixing. *Proc Natl Acad Sci USA* 103: 7228–7233
96. Vestad T, Marr D, Oakey J (2004) Flow control for capillary-pumped microfluidic systems. *J Micromech Microeng* 14:1503
97. Stiles T, Fallon R, Vestad T, Oakey J, Marr D, Squier J, Jimenez R (2005) Hydrodynamic focusing for vacuum-pumped microfluidics. *Microfluid Nanofluid* 1(3):280–283
98. Lee G, Chang C, Huang S, Yang R (2006) The hydrodynamic focusing effect inside rectangular microchannels. *J Micromech Microeng* 16:1024
99. Lee G, Hung C, Ke B, Huang G, Hwei B, Lai H (2001) Hydrodynamic focusing for a micromachined flow cytometer. *Trans ASME J Fluid Eng* 123(3):672–679
100. Wu Z, Nguyen N (2005) Hydrodynamic focusing in microchannels under consideration of diffusive dispersion: theories and experiments. *Sens Actuators B Chem* 107(2):965–974
101. Wu Z, Nguyen N (2005) Rapid mixing using two-phase hydraulic focusing in microchannels. *Biomed Microdevices* 7(1):13–20
102. Park H, Qiu X, Rhoades E, Korlach J, Kwok L, Zipfel W, Webb W, Pollack L (2006) Achieving uniform mixing in a microfluidic device: hydrodynamic focusing prior to mixing. *Anal Chem* 78(13):4465–4473
103. Nguyen N, Huang X (2005) Mixing in microchannels based on hydrodynamic focusing and time-interleaved segmentation: modelling and experiment. *Lab Chip* 5(11):1320–1326
104. Chang C, Huang Z, Yang R (2007) Three-dimensional hydrodynamic focusing in two-layer polydimethylsiloxane (PDMS) microchannels. *J Micromech Microeng* 17:1749
105. Simonnet C, Groisman A (2005) Two-dimensional hydrodynamic focusing in a simple microfluidic device. *Appl Phys Lett* 87:114104
106. Sundararajan N, Pio M, Lee L, Berlin A (2004) Three-dimensional hydrodynamic focusing in polydimethylsiloxane (PDMS) microchannels. *J Microelectromech Syst* 13(4):559–567
107. Yang R, Feeback D, Wang W (2005) Microfabrication and test of a three-dimensional polymer hydro-focusing unit for flow cytometry applications. *Sens Actuators A Phys* 118(2):259–267
108. Mao X, Lin S, Dong C, Huang T (2009) Single-layer planar on-chip flow cytometer using microfluidic drifting based three-dimensional (3D) hydrodynamic focusing. *Lab Chip* 9(11): 1583–1589
109. Mao X, Waldeisen J, Huang T (2007) “Microfluidic drifting” – implementing three-dimensional hydrodynamic focusing with a single-layer planar microfluidic device. *Lab Chip* 7(10): 1260–1262. <http://dx.doi.org/10.1039/B711155J>
110. Ottino J (1989) *The kinematics of mixing: stretching, chaos, and transport*. Cambridge University Press, Cambridge
111. Mengeaud V, Josserand J, Girault H (2002) Mixing processes in a zigzag microchannel: finite element simulations and optical study. *Anal Chem* 74(16):4279–4286
112. Jiang F, Drese K, Hardt S, Küpper M, Schönfeld F (2004) Helical flows and chaotic mixing in curved micro channels. *AIChE J* 50(9):2297–2305
113. Schönfeld F, Hardt S (2004) Simulation of helical flows in microchannels. *AIChE J* 50(4): 771–778
114. Chen H, Meiners J (2004) Topologic mixing on a microfluidic chip. *Appl Phys Lett* 84:2193
115. Liu R, Stremmer M, Sharp K, Olsen M, Santiago J, Adrian R, Aref H, Beebe D (2000) Passive mixing in a three-dimensional serpentine microchannel. *J Microelectromech Syst* 9(2): 190–197
116. Vijayendran R, Motsegood K, Beebe D, Leckband D (2003) Evaluation of a three-dimensional micromixer in a surface-based biosensor†. *Langmuir* 19(5):1824–1828
117. Lin Y, Gerfen G, Rousseau D, Yeh S (2003) Ultrafast microfluidic mixer and freeze-quenching device. *Anal Chem* 75(20):5381–5386
118. Stroock A, Dertinger S, Whitesides G, Ajdari A (2002) Patterning flows using grooved surfaces. *Anal Chem* 74(20):5306–5312

119. Hassell D, Zimmerman W (2006) Investigation of the convective motion through a staggered herringbone micromixer at low Reynolds number flow. *Chem Eng Sci* 61(9):2977–2985
120. Wang H, Iovenitti P, Harvey E, Masood S (2002) Optimizing layout of obstacles for enhanced mixing in microchannels. *Smart Mater Struct* 11:662
121. Bhagat A, Papautsky I (2008) Enhancing particle dispersion in a passive planar micromixer using rectangular obstacles. *J Micromech Microeng* 18:085005. <http://dx.doi.org/10.1088/0960-1317/18/8/085005>
122. Bhagat A, Peterson E, Papautsky I (2007) A passive planar micromixer with obstructions for mixing at low Reynolds numbers. *J Micromech Microeng* 17:1017
123. Yang J, Fang W, Tung K (2008) Fluids mixing in devices with connected-groove channels. *Chem Eng Sci* 63(7):1871–1881
124. Yang J, Huang K, Tung K, Hu I (2007) A chaotic micromixer modulated by constructive vortex agitation. *J Micromech Microeng* 17:2084. <http://dx.doi.org/10.1088/0960-1317/17/10/021>
125. Howell P, Mott D, Fertig S, Kaplan C, Golden J, Oran E, Ligler F (2005) A microfluidic mixer with grooves placed on the top and bottom of the channel. *Lab Chip* 5(5):524–530
126. Hong C, Choi J, Ahn C (2004) A novel in-plane passive microfluidic mixer with modified Tesla structures. *Lab Chip* 4(2):109–113
127. Sudarsan A, Ugaz V (2006) Fluid mixing in planar spiral microchannels. *Lab Chip* 6(1):74–82
128. Park S, Kim J, Park J, Chung S, Chung C, Chang J (2004) Rapid three-dimensional passive rotation micromixer using the breakup process. *J Micromech Microeng* 14:6
129. Long M, Sprague M, Grimes A, Rich B, Khine M (2009) A simple three-dimensional vortex micromixer. *Appl Phys Lett* 94:133501
130. Park J, Kim D, Kang T, Kwon T (2008) Improved serpentine laminating micromixer with enhanced local advection. *Microfluid Nanofluid* 4(6):513–523
131. Kim D, Lee S, Kwon T, Ahn C (2005) A serpentine laminating micromixer combining splitting/recombination and advection. *Lab Chip* 5(7):739–747. <http://dx.doi.org/10.1039/B418314B>
132. Wang L, Yang J (2006) An overlapping crisscross micromixer using chaotic mixing principles. *J Micromech Microeng* 16:2684. <http://dx.doi.org/10.1088/0960-1317/16/12/022>
133. Wang L, Yang J, Lyu P (2007) An overlapping crisscross micromixer. *Chem Eng Sci* 62(3):711–720
134. Kim S, Song Y, Skipper P, Han J (2006) Electrohydrodynamic generation and delivery of monodisperse picoliter droplets using a poly (dimethylsiloxane) microchip. *Anal Chem* 78(23):8011–8019
135. Lorenz R, Edgar J, Jeffries G, Chiu D (2006) Microfluidic and optical systems for the on-demand generation and manipulation of single femtoliter-volume aqueous droplets. *Anal Chem* 78(18):6433–6439
136. Quevedo E, Steinbacher J, McQuade D (2005) Interfacial polymerization within a simplified microfluidic device: capturing capsules. *J Am Chem Soc* 127(30):10498–10499
137. Handique K, Burns M (2001) Mathematical modeling of drop mixing in a slit-type microchannel. *J Micromech Microeng* 11:548
138. Nisisako T, Torii T, Takahashi T, Takizawa Y (2006) Synthesis of monodisperse bicolored janus particles with electrical anisotropy using a microfluidic Co flow system. *Adv Mater* 18(9):1152–1156
139. Song H, Bringer M, Tice J, Gerds C, Ismagilov R (2009) Experimental test of scaling of mixing by chaotic advection in droplets moving through microfluidic channels. *Appl Phys Lett* 83(22):4664–4666
140. Song H, Ismagilov R (2003) Millisecond kinetics on a microfluidic chip using nanoliters of reagents. *J Am Chem Soc* 125(47):14613–14619
141. Günther A, Jensen K (2006) Multiphase microfluidics: from flow characteristics to chemical and materials synthesis. *Lab Chip* 6(12):1487–1503



142. Shui L, Eijkel J, van den Berg A (2007) Multiphase flow in micro-and nanochannels. *Sens Actuators B Chem* 121(1):263–276
143. Sugiura S, Nakajima M, Seki M (2002) Effect of channel structure on microchannel emulsification. *Langmuir* 18(15):5708–5712
144. Okushima S, Nisisako T, Torii T, Higuchi T (2004) Controlled production of monodisperse double emulsions by two-step droplet breakup in microfluidic devices. *Langmuir* 20(23):9905–9908
145. Shui L, Eijkel J, van den Berg A (2007) Multiphase flow in microfluidic systems-control and applications of droplets and interfaces. *Adv Colloid Interface Sci* 133(1):35–49
146. Thorsen T, Roberts R, Arnold F, Quake S (2001) Dynamic pattern formation in a vesicle-generating microfluidic device. *Phys Rev Lett* 86(18):4163–4166
147. Yobas L, Martens S, Ong W, Ranganathan N (2006) High-performance flow-focusing geometry for spontaneous generation of monodispersed droplets. *Lab Chip* 6(8):1073–1079. <http://dx.doi.org/10.1039/B602240E>
148. Garstecki P, Fuerstman M, Stone H, Whitesides G (2006) Formation of droplets and bubbles in a microfluidic T-junction – scaling and mechanism of break-up. *Lab Chip* 6(3):437–446
149. Teh S, Lin R, Hung L, Lee A (2008) Droplet microfluidics. *Lab Chip* 8(2):198–220
150. Garstecki P, Fuerstman M, Whitesides G (2005) Nonlinear dynamics of a flow-focusing bubble generator: an inverted dripping faucet. *Phys Rev Lett* 94(23):234502
151. Bringer M, Gerds C, Song H, Tice J, Ismagilov R (1818) Microfluidic systems for chemical kinetics that rely on chaotic mixing in droplets. *Philos Trans R Soc Lond A Math Phys Eng Sci* 362:1087
152. Tice J, Lyon A, Ismagilov R (2004) Effects of viscosity on droplet formation and mixing in microfluidic channels. *Anal Chim Acta* 507(1):73–77
153. Pohar A, Plazl I, Žnidaršič-Plazl P (2009) Lipase-catalyzed synthesis of isoamyl acetate in an ionic liquid/n-heptane two-phase system at the microreactor scale. *Lab Chip* 9(23):3385–3390
154. Liao A, Karnik R, Majumdar A, Cate J (2005) Mixing crowded biological solutions in milliseconds. *Anal Chem* 77(23):7618–7625
155. Tung K, Li C, Yang J (2009) Mixing and hydrodynamic analysis of a droplet in a planar serpentine micromixer. *Microfluid Nanofluid* 7(4):545–557
156. Deshmukh A, Liepmann D, Pisano A (2000) Characterization of a micro-mixing, pumping, and valving system. In: *Proceedings 11th international conference on solid-state sensor and actuators (Transducers'01)*, Munich, Germany, 10–14 June 2001, pp 950–953
157. Deshmukh A, Liepmann D, Pisano A (2001) Continuous micromixer with pulsatile micro-pumps. In: *Proceedings IEEE solid-state sensor and actuator workshop*, Hilton Head Island, SC, 4–8 June 2000, pp 73–76
158. Fujii T, Sando Y, Higashino K, Fujii Y (2003) A plug and play microfluidic device. *Lab Chip* 3(3):193–197
159. Lim C, Lam Y, Yang C (2010) Mixing enhancement in microfluidic channel with a constriction under periodic electro-osmotic flow. *Biomicrofluidics* 4:014101
160. Lei K, Li W (2008) A novel in-plane microfluidic mixer using vortex pumps for fluidic discretization. *J Assoc Lab Automation* 13(4):227–236
161. Oddy M, Santiago J, Mikkelsen J (2001) Electrokinetic instability micromixing. *Anal Chem* 73(24):5822–5832
162. Yang R, Wu C, Tseng T, Huang S, Lee G (2005) Enhancement of electrokinetically-driven flow mixing in microchannel with added side channels. *Jpn J Appl Phys* 1 44(10):7634
163. Posner J, Santiago J (2006) Convective instability of electrokinetic flows in a cross-shaped microchannel. *J Fluid Mech* 555:1–42
164. Qian S, Bau H (2002) A chaotic electroosmotic stirrer. *Anal Chem* 74(15):3616–3625
165. Glasgow I, Batton J, Aubry N (2004) Electroosmotic mixing in microchannels. *Lab Chip* 4(6):558–562



166. Tang Z, Hong S, Djukic D, Modi V, West A, Yardley J, Osgood R (2002) Electrokinetic flow control for composition modulation in a microchannel. *J Micromech Microeng* 12: 870
167. Yan DG, Yang C, Miao JM, Lam YC, Huang XY (2009) Enhancement of electrokinetically driven microfluidic T-mixer using frequency modulated electric field and channel geometry effects. *Electrophoresis* 30(18):3144–3152
168. Lee H, Voldman J (2007) Optimizing micromixer design for enhancing dielectrophoretic microconcentrator performance. *Anal Chem* 79(5):1833–1839
169. Deval J, Tabeling P, Ho C (2002) A dielectrophoretic chaotic mixer. In: *Proceedings 15th international conference on micro electro mechanical systems*, Las Vegas, NV, 20–24 January 2002, pp 36–39
170. Goet G, Baier T, Hardt S (2009) Micro contactor based on isotachophoretic sample transport. *Lab Chip* 9(24):3586–3593. doi:[10.1039/b914466h](https://doi.org/10.1039/b914466h)
171. Paik P, Pamula V, Pollack M, Fair R (2003) Electrowetting-based droplet mixers for microfluidic systems. *Lab Chip* 3(1):28–33
172. Paik P, Pamula V, Fair R (2003) Rapid droplet mixers for digital microfluidic systems. *Lab Chip* 3(4):253–259
173. Fowler J, Moon H, Kim C (2002) Enhancement of mixing by droplet-based microfluidics. In: *Proceedings IEEE 15th international conference on micro electro mechanical systems*, Las Vegas, NV, 20–24 January 2002, pp 97–100
174. West J, Karamata B, Lillis B, Gleeson J, Alderman J, Collins J, Lane W, Mathewson A, Berney H (2002) Application of magnetohydrodynamic actuation to continuous flow chemistry. *Lab Chip* 2(4):224–230
175. Oh D, Jin J, Choi J, Kim H, Lee J (2007) A microfluidic chaotic mixer using ferrofluid. *J Micromech Microeng* 17:2077
176. Yang Z, Goto H, Matsumoto M, Maeda R (2000) Active micromixer for microfluidic systems using lead-zirconate-titanate (PZT)-generated ultrasonic vibration. *Electrophoresis* 21(1):116–119
177. Woias P, Hauser K, Yacoub-George E (2000) An active silicon micromixer for mTAS applications. In: van den Berg A, Olthuis W, Bergveld P (eds) *Proceedings micro total analysis systems symposium (μTAS2000)*, Enschede, The Netherlands, 14–18 May 2000, pp 277–282
178. Liu R, Yang J, Pindera M, Athavale M, Grodzinski P (2002) Bubble-induced acoustic micromixing. *Lab Chip* 2(3):151–157
179. Liu R, Lenigk R, Druyor-Sanchez R, Yang J, Grodzinski P (2003) Hybridization enhancement using cavitation microstreaming. *Anal Chem* 75(8):1911–1917
180. Jang L, Chao S, Holl M, Meldrum D (2007) Resonant mode-hopping micromixing. *Sens Actuators A Phys* 138(1):179–186
181. Ahmed D, Mao X, Shi J, Juluri B, Huang T (2009) A millisecond micromixer via single-bubble-based acoustic streaming. *Lab Chip* 9(18):2738–2741. <http://dx.doi.org/10.1039/B903687C>
182. Kim S, Wang F, Burns M, Kurabayashi K (2009) Temperature-programmed natural convection for micromixing and biochemical reaction in a single microfluidic chamber. *Anal Chem* 81(11):4510–4516
183. Lu L, Ryu K, Liu C (2002) A magnetic microstirrer and array for microfluidic mixing. *J Microelectromech Syst* 11(5):462–469
184. Mensing G, Pearce T, Graham M, Beebe D (1818) An externally driven magnetic micro-stirrer. *Philos Trans R Soc Lond A Math Phys Eng Sci* 362:1059
185. Huh Y, Park T, Lee E, Hong W, Lee S (2008) Development of a fully integrated microfluidic system for sensing infectious viral disease. *Electrophoresis* 29(14):2960–2969
186. Haeberle S, Brenner T, Schlosser H, Zengerle R, Durrée J (2005) Centrifugal micromixery. *Chem Eng Technol* 28(5):613–616
187. Chakraborty S, Balakotaiah V (2003) A novel approach for describing mixing effects in homogeneous reactors. *Chem Eng Sci* 58(3–6):1053–1061

188. Baldyga J, Bourne J, Hearn S (1997) Interaction between chemical reactions and mixing on various scales. *Chem Eng Sci* 52(4):457–466
189. Hessel V, Hardt S, Löwe H (2004) Chemical micro process engineering: fundamentals, modelling and reactions. Wiley-Vch, Weinheim
190. Karnik R, Gu F, Basto P, Cannizzaro C, Dean L, Kyei-Manu W, Langer R, Farokhzad O (2008) Microfluidic platform for controlled synthesis of polymeric nanoparticles. *Nano Lett* 8(9):2906–2912
191. Shestopalov I, Tice J, Ismagilov R (2004) Multi-step synthesis of nanoparticles performed on millisecond time scale in a microfluidic droplet-based system. *Lab Chip* 4(4):316–321
192. Chow A (2002) Lab on a chip: opportunities for chemical engineering. *AIChE J* 48(8):1590–1595
193. Jensen K (2001) Microreaction engineering – is small better? *Chem Eng Sci* 56(2):293–303
194. Mason B, Price K, Steinbacher J, Bogdan A, McQuade D (2007) Greener approaches to organic synthesis using microreactor technology. *Chem Rev* 107(6):2300–2318
195. Aoki N, Hasebe S, Mae K (2004) Mixing in microreactors: effectiveness of lamination segments as a form of feed on product distribution for multiple reactions. *Chem Eng J* 101(1–3):323–331
196. Chambers R, Fox M, Sandford G (2005) Elemental fluorine Part 18. Selective direct fluorination of 1, 3-ketoesters and 1, 3-diketones using gas/liquid microreactor technology. *Lab Chip* 5(10):1132–1139
197. Demello A (2006) Control and detection of chemical reactions in microfluidic systems. *Nature* 442(7101):394–402
198. Kestenbaum H, Lange de Oliveira A, Schmidt W, Schüth F, Ehrfeld W, Gebauer K, Löwe H, Richter T (2000) Synthesis of ethylene oxide in a catalytic microreactor system. *Stud Surf Sci Catal* 130:2741–2746
199. Surangalikh H, Ouyang X, Besser R (2003) Experimental study of hydrocarbon hydrogenation and dehydrogenation reactions in silicon microfabricated reactors of two different geometries. *Chem Eng J* 93(3):217–224
200. Huebner A, Sharma S, Srisa-Art M, Hollfelder F, Edel J, demello A (2008) Microdroplets: a sea of applications? *Lab Chip* 8(8):1244–1254
201. Li W, Young E, Seo M, Nie Z, Garstecki P, Simmons C, Kumacheva E (2008) Simultaneous generation of droplets with different dimensions in parallel integrated microfluidic droplet generators. *Soft matter* 4(2):258–262
202. Capretto L, Mazzitelli S, Balestra C, Tosi A, Nastruzzi C (2008) Effect of the gelation process on the production of alginate microbeads by microfluidic chip technology. *Lab Chip* 8(4):617–621
203. Nisisako T, Torii T (2008) Microfluidic large-scale integration on a chip for mass production of monodisperse droplets and particles. *Lab Chip* 8(2):287–293
204. Fair R (2007) Digital microfluidics: is a true lab-on-a-chip possible? *Microfluid Nanofluid* 3(3):245–281
205. Link D, Grasland Mongrain E, Duri A, Sarrazin F, Cheng Z, Cristobal G, Marquez M, Weitz D (2006) Electric control of droplets in microfluidic devices. *Angew Chem* 118(16):2618–2622
206. Krishnadasan S, Brown R, Demello A, Demello J (2007) Intelligent routes to the controlled synthesis of nanoparticles. *Lab Chip* 7(11):1434–1441
207. Voloshin Y, Halder R, Lawal A (2007) Kinetics of hydrogen peroxide synthesis by direct combination of H<sub>2</sub> and O<sub>2</sub> in a microreactor. *Catal Today* 125(1–2):40–47



<http://www.springer.com/978-3-642-23049-3>

Microfluidics

Technologies and Applications

Lin, B. (Ed.)

2011, XII, 344 p., Hardcover

ISBN: 978-3-642-23049-3